Journal of Experimental Psychology:
Human Perception and Performance
1995, Vol. 21, No. 1, 32-53

0096-1523/95/$3.00

Minimum-Jerk, Two-Thirds Power Law, and Isochrony: Converging Approaches to Movement Planning

Paolo Viviani
Université de Genève
and Istituto di Neuroscienze e Bioimmagini

Tamar Flash
Weizman Institute of Science

Two approaches to the study of movement planning were contrasted. Data on the drawing of complex two-dimensional trajectories were used to test whether the covariations of the kinematic and geometrical parameters of the movement formalized by the two-thirds power law and by the isochrony principle (P. Viviani & R. Schneider, 1991) can be derived from the minimum-jerk model hypothesis (T. Flash & N. Hogan, 1985). The convergence of the 2 approaches was satisfactory insofar as the relation between tangential velocity and curvature is concerned (two-thirds power law). Global isochrony could not be deduced from the optimal control hypothesis. Scaling of velocity within movement subunits can instead be derived from the minimum-jerk hypothesis. The implications vis-à-vis the issue of movement planning are discussed with an emphasis on the representation used by the motor control system for coding the intended trajectories.

Because of the flexibility and redundancy of the neuromuscular and skeletal systems, many motor goals can be achieved using different combinations of elementary movements. Differences may be quantitative—for example, one position in space can be reached with the fingertip using various sets of angles between the articular joints; one trajectory can be traced with different velocity profiles—or qualitative—for example, a handle can be turned using either the overhand or the underhand grip; horses can reach certain speeds by either trotting or galloping. Although humans do sometimes take advantage of such freedom, there is often evidence of strong biases favoring one solution over all alternatives (Kay, 1988). Motor theorists believe that we would make a significant step toward elucidating the logic of motor control if we were to understand the constraining principles responsible for the reduction of the available degrees of freedom (Jordan, 1990; Whiting, 1984). However, it is not clear yet (cf. Rosenbaum, Vaughan, Jorgensen, Barnes, & Stewart, 1993) whether one conceptual framework can subsume qualitative differences in motor strategies under a quantitative theory. In this article, we deal exclusively with the special but important case in which the goal is uniquely defined by the motion of a well-identified endpoint (as in writing or drawing), and differences between alternative motor solutions are clearly quantitative. In particular, we address how geometrical and kinematic aspects of endpoint movements are specified and what is the nature of the constraints that intervene in the specification.

Several approaches have been devised to tackle this question. Some of them share a set of assumptions that, for sake of reference, we identify collectively as the motor program view. A motor program is generally defined as the central representation of a sequence of motor actions that can lead to a patterned movement in the absence of feedback (Keele, 1981). Generality and flexibility can be achieved if one introduces in the definition of program the distinction between structural aspects of the intended action (that are assumed to be invariant and stored in memory) and parameters (total duration of the action, amount of force used in execution, choice of the muscular synergies, etc.) that are specified only at the time of execution (Schmidt, 1975, 1976, 1987). The nature of the structural, invariant information is still debated. Some authors (e.g., Stelmach, Mullins, & Teulings, 1984; Wing, 1978, 1979, 1980) suggest that the plan is a preset temporal sequence of activations of agonist and antagonist muscles; recent neurophysiological (Alexander & Crutcher, 1990a, 1990b; Crutcher & Alexander, 1990; Kalaska, Cohen, Hyde, & Prud'homme, 1989; Kalaska, Cohen, Prud'homme, & Hyde, 1990) and behavioral data (for a review, see Van Galen, 1991) are instead compatible with the hypothesis that spatial variables are represented in the motor plan. In either case, it is a basic tenet of the motor program view (at least for such complex, learned gestures as handwriting or drawing; Ellis, 1988) that some internal representation of the intended trajectory is available to the implementation stage prior to the inception of movement; moreover, it is also often assumed that the spatial relationships observed in overt behavior correspond isomorphically to identifiable features of this internal representation. In particular, some key geometrical features of

Paolo Viviani, Department of Psychobiology, Université de Genève, Geneva, Switzerland, and Istituto di Neuroscienze e Bioimmagini, Milan, Italy; Tamar Flash, Weizman Institute of Science, Rehovot, Israel.

This work was partly supported by Fonds National de la Recherche Suisse Research Grant 31.25265.88 (MUCOM ESPRIT Project) to Paolo Viviani and by U.S.-Israel Binational Science Foundation Grant 8800141 to Tamar Flash. We are grateful to Sharon Yalov for her contribution to the early phase of the project.

Correspondence concerning this article should be addressed to Paolo Viviani, Department of Psychobiology, Faculty of Psychology and Educational Sciences, Université de Genève–9, Route de Drize, 1227 Carouge, Switzerland. Electronic mail may be sent to viviani@cgeuge51.

the trajectory—such as its length, or the presence of closed loops—are supposed to be traceable to specific aspects of the motor plan. Finally, the fact that the temporal structure of the movement can be kept relatively invariant across voluntary changes in tempo and size (ratiomorphic scaling) is sometimes interpreted by the motor program view as evidence that kinematic variables are constrained to some extent by the geometrical properties of the intended trajectory (Teulings, Mullins, & Stelmach, 1986).

Other approaches to movement planning depart more or less drastically from the premises that characterize the motor program view. Although they differ in several important respects, many of these approaches share the tenet that overt features of the movement (both geometrical and kinematic alike) are concurrently specified by a few basic principles that preside over the working of the motor control system. Thus, for instance, the so-called pattern dynamics approach (cf. Haken & Wunderlin, 1990; Kelso & Schöner, 1987; Kelso, Schöner, Scholz, & Haken, 1987; Saltzman & Kelso, 1987; Schöner & Kelso, 1988) holds that the coordination of bimanual oscillations, the stability of coordination patterns, and the phase transitions that occur between stable modes of coordination should be construed as nonlinear dynamic phenomena involving collective variables, that is, low-dimensional quantitative descriptors of the order or relations among components. Discrete movements can also be investigated within the same framework by identifying their intrinsic dynamics in terms of initial and target postural states (Schöner, 1990).

Another example of alternative approach is the so-called mass-spring theory of handwriting (Hollerbach, 1981; Kelso, 1981), which argues that harmonic oscillations represent the most fundamental mode of action of viscoelastic biomechanical systems, and that a rich variety of distinctive features of cursive letters (e.g., the presence of closed loops, the slant and height of strokes, the sense of rotation, etc.) can be selected by controlling stiffness and viscosity of orthogonally arranged (second-order) dynamic systems. Finally, cost-minimization models (one of which will be described later in greater detail) represent yet another instance of departure from the motor program view inasmuch as they postulate that movement planning is based on a global principle of optimal control, and that no complete blueprint exists for the generation of the movement. For instance, the minimum spatial deviation model (Jordan, Flash, & Arnon, in press) assumes that point-to-point movements result from the implicit constraint that the trajectory deviates as little as possible from a straight line. It can be shown that minimizing a cost-function that takes into account the total deviation, in conjunction with the constraints that arise from the dynamical properties of the neuromuscular system, suffices to specify the law of motion of the movement. Over and above the variety of mechanisms invoked to explain specific motor behaviors, the feature that all these approaches share is the low dimensionality of the control space wherein the movement plan is coded: Because many aspects of the movement's complexity are supposed to result from the implementation process, the plan need not bear any isomorphic relationship with observable properties of the resulting gesture.

In the face of the considerable divergence of the respective premises, the motor program view would a priori seem incompatible with any of these competing views. However, if the implementation of these different ideas failed to produce contrasting predictions concerning the execution of some reasonably complex motor task, one could suspect that differences are more terminological than substantive, and that some sort of integration can be achieved. In this article, we explore this possibility by contrasting two specific strategies for investigating movement planning that have been independently pursued by the authors over the last few years; one strategy is inspired by the motor program view, the other by the concept of global optimization. Although neither of them can claim to be representative of the entire conceptual domain to which it is associated, both present some prototypical features of the respective camp. Thus, we hope that the conclusions of our joint effort of clarification may have some relevance beyond the context of this study.

The article is organized as follows. First, we outline the two strategies under examination, as well as a few basic results obtained with each of them. Then, after summarizing a recent critical appraisal of their relationship (Wann, Nimmo-Smith, & Wing, 1988), we present the motivations for taking up the issue once more. Next, we describe an experiment that provides the empirical basis for evaluating the convergence between the two strategies. A subsequent section analyzes quantitatively the manner in which each of them deals with the same body of data. Finally, we discuss the level of integration that it has been possible to achieve, as well as the significance of the remaining discrepancies.

Explicit Versus Implicit Constraints

It is still open to debate whether the central nervous system (CNS) plans hand movements in terms of angular (intrinsic) coordinates at the arm joints (e.g., Lacquaniti & Soechting, 1982; Soechting & Lacquaniti, 1981; Soechting, Lacquaniti, & Terzuolo, 1986), or in terms of body-centered (extrinsic) coordinates of the relevant end point (e.g., Flash & Hogan, 1985; Georgopoulos, Kalaska, Caminiti, & Massey, 1982; Georgopoulos, Kettner, & Schwartz, 1988; Morasso, 1981). However, the two strategies contrasted here adopt the same point of view in this debate, namely, that the motor control system represents hand position in space in an extrinsic system of reference. Thus, in the upcoming presentation we are concerned exclusively with the distal variables that characterize endpoint motions. Moreover, we will restrict the analysis to the special case of planar movements.

A planar point movement can be described in at least three equivalent ways:

1. It can be described by providing the time course of the coordinates $[x = x(t), y = y(t)]$.

2. It can be described by specifying both the geometrical form of the trajectory,[1] which in turn is described by the parametric equations G: $[x = x(s), y = y(s)]$ (where s is the curvilinear coordinate), and the law of motion M: $\{s = s(t)\}$ which indicates the length of the segment of trajectory spanned from motion onset ($t = 0$) to time t.
3. It can be described by specifying the radius of curvature $R(s)$ of the trajectory and the tangential velocity of the point $V(s) = ds/dt$, both as a function of curvilinear coordinate (to within a location parameter the function $R(s)$ uniquely defines a trajectory [Guggenheimer, 1963]).

In the domain of kinematics no relation needs to exist between G and M or R and V: a trajectory can be traced with any law of motion and, conversely, a specific law of motion can be followed along any trajectory. The situation is different in the domain of dynamics (i.e., when one takes into account the forces that generate the movement). In fact, the time course of the forces, in conjunction with Newton's equation, specifies jointly the trajectory and the law of motion; thus, G and M (as well as R and V) are mutually constrained in a manner that depends uniquely on the driving forces. It follows that, if a principled relationship exists between G and M (or, equivalently, between the functions R and V), which is invariant for a class of movements generated by one controlling system, this relationship must be the reflection of a general rule that the system follows in planning the forces. Ultimately, any consistent pattern of covariation between quantities related to geometry and kinematics is likely to provide a clue for understanding the logic of the controller.

Two-Thirds Power Law and Isochrony

A research program carried out in recent years has investigated two such patterns of covariation (Lacquaniti, Terzuolo, & Viviani, 1983, 1984; Viviani & Cenzato, 1985; Viviani & McCollum, 1983; Viviani & Schneider, 1991; Viviani & Terzuolo, 1980, 1982). The first principle formalizes a local constraint between geometry and law of motion, that is, a constraint that involves the properties of the movement at any one point in time. It has long been observed that curvature and velocity of endpoint hand movements are related (Binet & Courtier, 1893; Jack, 1895). Early attempts to formulate this observation mathematically (Lacquaniti et al., 1983) led to a simple relation between curvature ($C = 1/R$) and angular velocity ($A = V/R$): $A = K\,C^{2/3}$ (two-thirds power law), valid only for a certain class of movements. The most recent formulation of the relation between curvature and velocity (Viviani & Schneider, 1991) extends the validity of the original law on three counts: (a) It covers a wider class of movements, including those composed of identifiable units of motor actions; (b) it deals satisfactorily with points of inflection; and (c) it takes into account certain aspects of the maturation of motor control in the course of development.

The new formulation relates the radius of curvature at any point s along the trajectory with the corresponding tangential velocity:

$$V(s) = K(s)\left(\frac{R(s)}{1 + \alpha R(s)}\right)^{\beta} \quad \alpha \geq 0,\ K(s) \geq 0. \qquad (1)$$

In adults, the exponent β takes values close to ⅓; the constant α ranges between 0 and 1, depending on the average velocity (Viviani & Stucchi, 1992). The multiplicative function $K(s)$ appearing in this equation has been termed the *velocity gain factor;* it depends on the length of the trajectory but not on its form. Although we have noted explicitly the dependency of K on the curvilinear coordinate s, the analysis of complex movements has shown that this term can be approximated in many cases by a piece-wise constant function (Viviani, 1986; Viviani & Cenzato, 1985). When $\beta = ⅓$, $\alpha = 0$ and $K(s) =$ constant, the new formulation is mathematically equivalent to its simpler, original version; thus, for the sake of consistency, Equation 1 is also referred to as the two-thirds power law.

The second covariance principle to be considered here is known as the isochrony principle. It is an old observation that average velocity of point-to-point movements increases with the distance between the points and, therefore, that movement duration is only weakly dependent on movement extent (Binet & Courtier, 1893; Derwort, 1938; Fitts, 1954; Freeman, 1914). More recent studies (Viviani, 1986; Viviani & McCollum, 1983; Viviani & Schneider, 1991) have shown that a similar phenomenon is present in almost any type of movement, periodic and aperiodic, regular and extemporaneous. In all cases the relative constancy of movement duration results directly from the empirical fact that the average velocity covaries with the linear extent of the trajectory. In particular, changing the scale at which one traces a given trajectory produces a similar change in the average velocity.

The two-thirds power law described above suggests a way of factoring out this change into two components. By taking the logarithms of both sides of Equation 1, substituting $C(s)$ for $1/R(s)$, and averaging over the entire length L of the path one obtains:

$$\frac{1}{L}\int_0^L \log[V(s)]ds = \frac{1}{L}\int_0^L \log[K(s)]ds + \frac{\beta}{L}\int_0^L \log\{1/[C(s) + \alpha]\}ds \qquad (2)$$

The left term in this equation is an increasing function of the average velocity; the first term on the right side is an increasing function of the average velocity gain; finally, the second term on the right is a decreasing function of the average curvature of the trajectory. Studies (Viviani & Cenzato, 1985; Viviani & Schneider, 1991) have shown that

[1] In robotics the term *trajectory* is sometimes used to denote collectively all kinematic variables that characterize a point motion, the term *path* being instead reserved to denote the geometrical form of the motion. In this article we adhere to the terminology adopted in rational mechanics.

the average gain in turn is an increasing function of the length L. Moreover, for any given form of the trajectory, average curvature scales inversely with the overall size of the movement. Thus, the modulation of the average velocity is the sum of two effects, one mediated by the velocity gain, the other related to the distribution of curvature along the path (for a discussion of the relative weight of these effects, see Viviani & Cenzato, 1985, and Viviani & Schneider, 1991). It has been argued (Viviani & Schneider, 1991) that these two contributions to the relative invariance of movement duration pertain to distinct aspects of motor planning, and that the term *isochrony* is best used to denote only the empirical (and so far unexplained) fact that the velocity gain is sensitive to the length of the path, rather than the overall covariation of average velocity with length.

A connection can be established between the phenomenon of isochrony and the decomposition of complex movements into units of motor action. Viviani (1986) suggested that all portions of a movement over which the velocity gain factor K is approximately constant (see above) correspond to relatively autonomous chunks of motor planning. The number and size of the units defined by this criterion depend on the nature of the movement as well as on the form of the trajectory. For instance, in the case of simple periodic motions, such as the continuous tracing of an ellipse, K is constant throughout; thus, there is only one identifiable unit that coincides with a complete cycle of movement. When tracing more elaborate closed patterns that contain identifiable figural elements (such as, for instance, the two loops in patterns T_1 and T_3 in Figure 2), the trajectory is typically decomposed in several units that correspond to these elements. Finally, in the case of very complex and nonperiodic movements, such as free scribbling, the segmentation into units occurs primarily at the points of inflection of the trajectory where the sense of rotation of the movement is inverted (Schneider, 1987).

Identifying the units of motor action by a criterion that involves the velocity gain factor is justified by the observation that average velocity within units is well predicted by the linear extent of the corresponding portions of trajectory.[2] In other words, the same phenomenon of isochrony that applies to the entire trajectory is also observed within units (the average velocity for the entire movement being itself a weighted mean of the individual averages). In both cases, the fact that velocity is modulated by a global geometrical quantity (the linear extent of the path) even before the trajectory is fully executed, suggests that an estimate of this quantity is available to the motor control system as part of the internal representation of the intended movement.

The factorization of velocity into two multiplicative factors suggested by the two-thirds power law (see above) applies also within units of motor actions where the velocity gain is approximately constant. Moreover, it can be shown that the dependency of the gain on the length of the path, which has been argued to be the most direct expression of the phenomenon of isochrony, is also present within units and corresponds to a local form of isochrony (Schneider, 1987). Specifically, let s_1 and s_2 be the curvilinear coordinates of the endpoints of a unit. It has been demonstrated (Schneider, 1987; see also Figure 1 in Viviani & Stucchi, 1992, and Figure 5B of the present article) that the empirical linear regression (in log units):

$$\log\left[\frac{1}{s_2 - s_1}\int_{s_1}^{s_2} K(s)ds\right] = \log K_0 + \delta\log(s_2 - s_1) \quad (3)$$

between the linear extent of the unit $(s_2 - s_1)$ and the corresponding average gain (left-sided integral) affords a satisfactory approximation to the data. Thus, the weak dependence of movement time on trajectory length is mostly due to the modulation of the velocity gain empirically described by Equation 3. The interplay between the modulation of the average velocity gain by the total length of the trajectory (global isochrony), and the modulation within units of motor action (local isochrony) is a complex problem that is not fully understood yet.

Minimum-Jerk Model

In summary, the line of research outlined above hinges on the assumption that (a) a spatial plan is available to the motor control system prior to the inception of the movement, and (b) many temporal and kinematic aspects of the action are explicitly constrained by the geometrical properties of the actual expected trajectory. Thus, whereas neither the two-thirds power law nor the isochrony principle addresses directly the problem of trajectory formation, both adhere on this issue to the premises that characterize the motor program view. By contrast, in some approaches to movement planning that break away from the motor program tradition, the necessary dissipation of the degrees of freedom results from constraints that are set at a much more global level inasmuch as they are supposed to correspond to general qualitative properties of the motor system. In particular, several authors have investigated the consequences of assuming that point-to-point movements comply with some global minimum-cost condition (Flash & Hogan, 1985; Hasan, 1986; Hogan, 1984; Hollerbach, 1977; Nagasaki, 1989; Nelson, 1983; Uno, Kawato, & Suzuki, 1989; Wann et al., 1988). Minimum-jerk modeling is a representative instance of this line of research. A formal mathematical description of the minimum-jerk model is provided in Flash and Hogan (1985) and Edelman and Flash (1987). It suffices here to sketch the main points.

Barring particular overriding circumstances, natural movements—and, more markedly, hand movements—tend to be smooth and graceful. One can then postulate that this characteristic feature corresponds to a design principle, or, in other words, that maximum smoothness is a criterion to which the motor system abides in the planning of end-point movements (Hogan & Flash, 1987). It is a mathematical fact that this constraint is so powerful that it can be turned into

[2] The situation is actually slightly more complex because of the presence of coupling between contiguous units (Viviani & Cenzato, 1985). This point will be taken up again in the discussion.

a motor recipe. To this end, one defines a cost function *CF* that is proportional to the mean square of the jerk (derivative of the acceleration):

$$CF = \tfrac{1}{2}\int_{t_1}^{t_2}\left[\left(\frac{d^3x}{dt^3}\right)^2 + \left(\frac{d^3y}{dt^3}\right)^2\right]dt \qquad (4)$$

and stipulates that the movement is "maximally smooth" if the corresponding parametric equations minimize the cost *CF*. It can be shown that there is only one pair of parametric equations that simultaneously satisfy this minimum condition and an appropriate set of boundary conditions.

In essence, then, the minimum-jerk model postulates that, among all possible solutions for generating a trajectory, the motor control system selects precisely this unique pair. In the case that is relevant here, namely, that in which one wants to go from an initial point $Q_1 = (x_1, y_1)$ to a final point $Q_3 = (x_3, y_3)$ by way of an intermediate position $Q_2 = (x_2, y_2)$, the selection process, framed as an optimal control problem with interior point equality constraints (Bryson & Ho, 1975), yields a closed analytical solution. The horizontal and vertical components of the movement are both expressed as fifth-order, polynomial functions of time:

$$x(t) = \sum_{k=0}^{5} c_{kx}t^k + p_{1x}(t - t_2)_+^4 + p_{2x}(t - t_2)_+^5$$

$$y(t) = \sum_{k=0}^{5} c_{ky}t^k + p_{1y}(t - t_2)_+^4 + p_{2y}(t - t_2)_+^5$$

$$(t - t_2)_+ = \begin{cases} t - t_2 & \text{if } t \geq t_2 \\ 0 & \text{if } t < t_2 \end{cases} \qquad (5)$$

where t_2 is the via-point passage time. The coefficients $\{c_{kx}, c_{ky}; k = 0, 5\}$, p_{1x}, p_{2x}, p_{1y}, and p_{2y} that appear in Equation 5 can be determined on the basis of the following set of boundary conditions: time, position, velocity and acceleration at Q_1 and Q_3, and position and velocity (or just position) at Q_2. The solution is invariant with respect to rotations and translations of the positions Q_1, Q_2, and Q_3; moreover, it is time homogeneous and scalable: changes in time scale leave the trajectory unaffected and are reflected proportionally in the kinematic parameters. It must be emphasized that passage time t_2 at the via-point is also determined jointly by the boundary and minimum conditions. Thus, the model makes quantitative predictions on the internal temporal structure of the movement. Specifically, by predicting how the relative duration $(t_2 - t_1)/(t_3 - t_1)$ of the first part of the movement (up to the via-point) varies as a function of the corresponding relative length of the trajectory $(s_2 - s_1)/(s_3 - s_1)$, one can test the ability of the model to simulate the phenomenon of local isochrony. These predictions were found to be in excellent agreement with the experimental results (Flash & Hogan, 1985) and, more generally, with the phenomenon of within-movement isochrony described by the empirical regression 3.

The minimum condition on movement derivatives affords considerable morphogenetic power. Even with a single via-point constraint, a great variety of curved trajectories can be generated through an appropriate choice of boundary conditions. Figure 1 illustrates this point with a representative example. Even more complex patterns can be obtained by chaining a sufficient number of point-to-point trajectories. Realistic simulations of handwriting derived from an optimum principle similar to the one embodied in the minimum-jerk model were obtained by Edelman and Flash (1987), who assumed that the instructions for complex movements (such as the writing of a letter string) are coded as a sequence of boundary conditions, each of which specifies completely the generation of successive segments of the trajectory. In agreement with the general philosophy of this type of approach, the CNS is supposed to represent handwriting and drawing in a high-level language, leaving many aspects of the actual result to the implementation stage. Thus, the format of the internal representation is far more compact and, at the same time, far more opaque than that typically postulated by the motor program view. Finally, we recall that, although an earlier version of the model was meant to describe actual movements, in later work (Flash, 1987, 1990) it has been argued that the minimum-jerk solution may describe an internal representation of the desired movement (equilibrium trajectory). We elaborate on this suggestion in the Discussion section.

Previous Work and Goal of the Project

A recent study (Wann et al., 1988) addressed the question of whether the dependency of velocity on curvature can be derived from a minimum-cost principle. Using data on the continuous tracing of ellipses by adult subjects, these authors argued the following points:

1. The two-thirds power law is a restatement of the general notion that many two-dimensional movements can be construed as the result of coupling two orthogonal harmonic motions. Therefore, the law is neither more significant nor more accurate than this simple oscillatory model.
2. Even in the most favorable case (i.e., when considering elliptical trajectories), there are asymmetries in the movement that significantly violate the two-thirds power law.
3. The hypothesis that the CNS seeks to minimize a cost function related to "jerkiness" implies a covariation between velocity and curvature that is commensurate with the empirical data. However, contrary to the assumption of Flash and Hogan's (1985) model, the cost function cannot be expressed by kinematic quantities only. Perceived jerkiness must relate in some way to the action of dynamic variables.
4. This revised minimization model provides a good account of human behavior under relaxed conditions. As such, and within these limits, it supersedes previous models.

Points 1 and 2 above have been discussed at length in a recent article (Viviani & Schneider, 1991). In particular, the analysis of the development of motor control in young children has demonstrated that, across ages, velocity and curvature are always related by a power function. However, the exponent of the function varies in the course of puberty and attains the value ⅓ found in adults only after the age of 12. The simple oscillatory model for the generation of

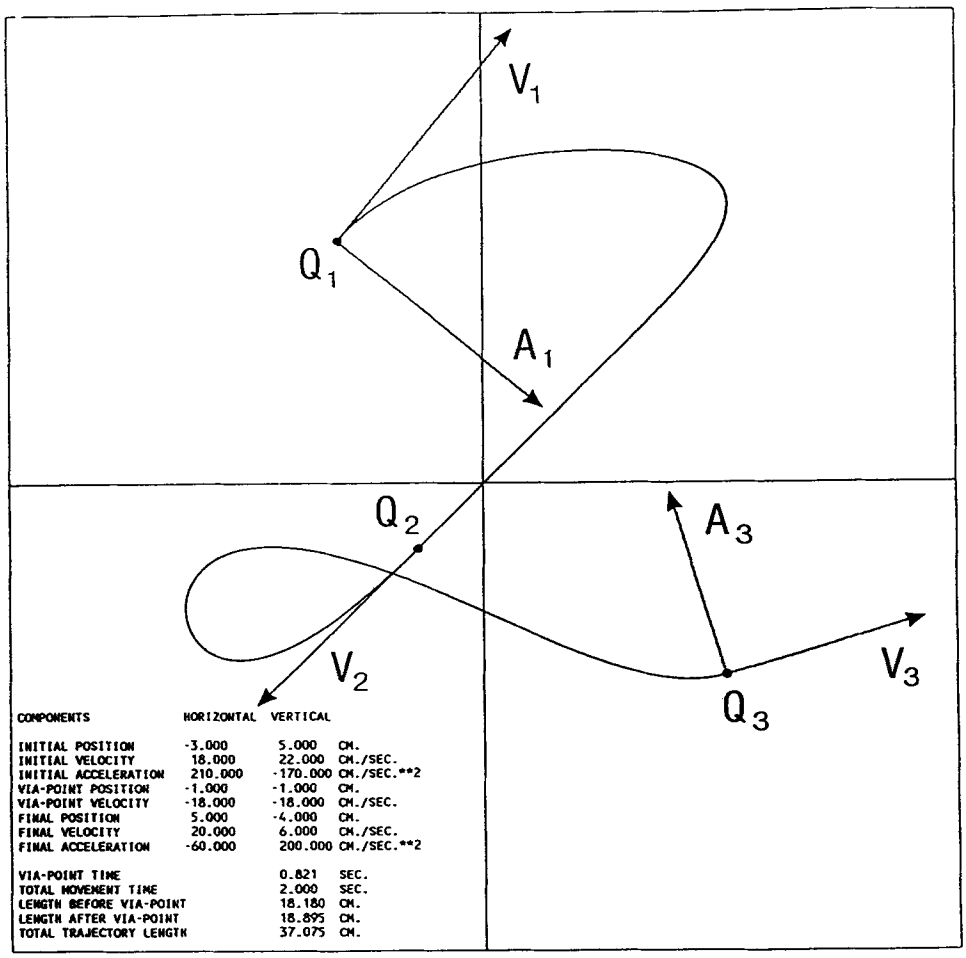

Figure 1. Morphogenetic capability of the minimum-jerk model. This is an example of the complex trajectories that can be generated by the model. Given an initial point (Q_1), a final point (Q_3), and a mandatory via-point (Q_2), a variety of trajectories can be obtained by choosing appropriately the kinematic boundary conditions. In this example the indicated velocity (V_1, V_2, V_3) and acceleration (A_1, A_2) vectors, as well as the imposed duration of the movement, induce the presence of a loop in the trajectory. Because the model is time-scalable (see text), the same trajectory can be executed in any specified amount of time, provided that velocities and accelerations are scaled proportionally.

elliptic movement instead predicts that the exponent of the power function is always ⅓ and is therefore at variance with these developmental data. Points 3 and 4 address issues that are directly relevant to our own program. Among others, they raise the question of how broad the range of phenomena should be that one takes into account when contrasting different approaches to the study of movement, and, relatedly, the question of what kind of database is adequate for carrying out this contrast. Because of the relation that exists between the two-thirds power law and isochrony (see above), we have adopted the view that the analysis of these two empirical principles should not be dissociated. We believe that the results obtained with motor tasks as simple as elliptic tracing studied by Wann et al. (1988) cannot provide the necessary discriminating power. The reason is twofold. On the one side, ellipses are generally traced by adults in such a way that the horizontal and vertical components of the movement are hard to distinguish from sine and cosine functions of time. This mode of generation is predicted by several models of control, including those, like the mass-spring model, that are conceptually quite distinct from both formalisms discussed here, and from Wann et al.'s model. On the other side, ellipses and other simple closed trajectories are normally traced as a unit (see above); thus, they provide no way of discriminating between local and global isochrony. The movements performed in our experiments overcome these limitations because their components are more complex than harmonic functions, and because the presence of clearly identifiable geometrical subunits is likely to induce a segmentation of the execution into distinct units of motor action.

The task proposed in our experiments, continuous tracing of three complex, closed trajectories, was designed to highlight those aspects of motor performance on which the two approaches to be contrasted make quantitative predictions. Two of the patterns contain similar loops that are concatenated with and without points of inflection (one pattern requires an inversion of the sense of rotation; the other does not). By changing the relative size of the loops while keeping the rhythm of execution (and, in one case, the total perimeter) constant, one can investigate the phenomena of local and global isochrony. The third pattern has a fourfold symmetry; by having subjects trace it at different rhythms, one can investigate the scaling properties of the movement. The three patterns present large variations in curvature, which permits one to quantify accurately the covariation between this geometrical parameter and the velocity. Finally, all patterns can be generated accurately by the minimum-jerk model; thus, a rigorous three-way comparison is possible between the kinematics predicted by the model, that predicted by the two-thirds power law, and the one that is actually measured.

Method

Subjects and Apparatus

Three right-handed men (S_1, S_2, and S_3) from the staff of P. Viviani's laboratory in Geneva volunteered as subjects. They were 35, 33, and 45 years old, respectively. The coordinates of drawing movements were recorded with a digitizing table (Numonics Corporation, Montgomeryville, PA; Model 2200-0.60TL.F; nominal accuracy: 0.01 mm; temporal resolution: 200 samples/s) placed horizontally in front of the sitting subjects. The writing implement of the table resembled a normal ballpoint pen but did not leave a visible trace. The model curves to be traced (templates) were drawn on standard-sized (A4) white sheets placed on the table.

Material

Three types of closed mathematical curves were used as templates: asymmetric lemniscate (T_1), cloverleaf (T_2), and oblate limaçon (T_3). Figure 2 illustrates one representative instance of each template. It also provides the corresponding general parametric equations. Absolute and relative sizes of the curves are specified by the constants a, b, and c in the equations. Three versions of T_1 and T_3 were tested, each corresponding to a different ratio between the linear extent of the large (P_1) and small (P_2) loops present in these curves. For template T_1 the total linear extent P_T was constant (48 cm). The ratio $r = P_1/P_2$ could take the values $r_1 = 1$ (T_{11}: $P_1 = P_2 = 24$ cm), $r_2 = 2$ (T_{12}: $P_1 = 32$ cm; $P_2 = 16$ cm), and $r_3 = 3$ (T_{13}: $P_1 = 36$ cm; $P_2 = 12$ cm). The values of the constants a and b corresponding to these size specifications were computed numerically with a simplex minimization algorithm (T_{11}: $a \leq 10^{-6}$; $b \geq 10^6$; ab = 9.1531; T_{12}: a = 3.2645; b = 2.7981; T_{13}: a = 4.9200; b = 1.8489). The total horizontal extent of the curve ($E_x = 2ab$) was almost identical in the three cases (T_{11}: $E_x = 18.31$ cm; T_{12}: $E_x = 18.27$ cm; T_{13}: $E_x = 18.19$ cm). The three versions of T_3 were defined as follows. The rightmost and leftmost points of the curve are reached for $\Theta = 0$ and $\Theta^* = \cos^{-1}(-1/4b)$. The difference between the abscissas of these two points is $E_x = a(4b + 1)^2/8b$. The ordinate y_{max} of the uppermost point of the curve is also a known function of b and c. P_1 and P_2 were defined as twice the length of the curve corresponding to the parametric intervals ($0 \leq \Theta \leq \Theta^*$) and ($\Theta^* \leq \Theta \leq \pi$), respectively. The eccentricity of the outer loop was defined as $\Sigma = [1 - 4(y_{max}/E_x)^2]^{1/2}$. For any choice of values of P_1, Σ, and $r = P_1/P_2$, the three constants appearing in the equations of the curve are uniquely defined. The values $P_1 = 45$ cm and $\Sigma = 0.9$ were fixed for the three versions of the template. The ratio $r = P_1/P_2$ could take the values $r_1 = 3/2$ (T_{31}: $P_2 = 30$ cm; $P_T = 75$ cm), $r_2 = 2$ (T_{32}: $P_2 = 22.5$ cm; $P_T = 67.5$ cm), and $r_3 = 3$ (T_{33}: $P_2 = 15$ cm; $P_T = 60$ cm). The values of a and b and c corresponding to these size specifications were again computed numerically (T_{31}: a = 3.3138; b = 2.4236; c = 1.3504; T_{32}: a = 5.0020; b = 1.4254; c = 1.9772; T_{33}: a = 6.7031; b = 0.9105; c = 2.5801). In this case also the total horizontal extent of the figure was almost independent of r (T_{31}: $E_x = 19.55$ cm; T_{32}: $E_x = 19.70$ cm; T_{33}: $E_x = 19.83$ cm). Only one T_2 template was used (a = 9.6 cm, $E_x = 8a/3\sqrt{3} = 14.75$ cm). The total linear extent of T_2 can be expressed in terms of the complete elliptic integral of the second kind E: $P_T = 8aE(3/4)$ and was equal to 93.00 cm.

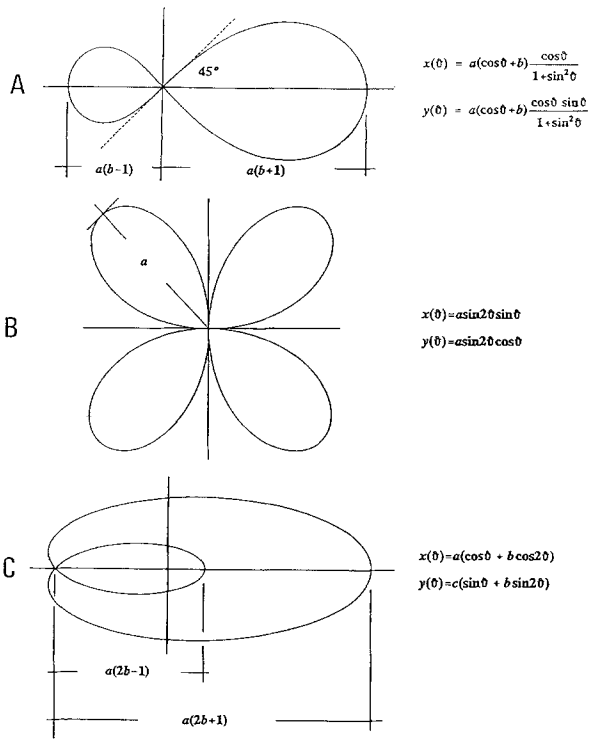

Figure 2. Templates used for the experiments. Row A: asymmetric lemniscate (T_1); Row B: cloverleaf (T_2); Row C: oblate limaçon (T_3). Each curve is described mathematically by the indicated parametric equations. By specifying the parameters *a*, *b*, and c in these equations as explained in the text, one can control the absolute and relative sizes of these templates.

Task and Procedure

The task consisted of tracing each version of the templates freely and continuously. T_1 was traced counterclockwise for the

large loop and clockwise for the small loop. T_2 and T_3 were traced counterclockwise. Movements were recorded for 10 s. The experimenter started the recording after a few cycles of movement during which subjects reached a stable pace. Subjects were tested in a single session. Sessions were divided into three phases, one for each type of template, with short periods of rest between phases. Each phase comprised a series of nine recordings. For T_1 and T_3 the series consisted of three repetitions for each version of the templates. Recording sequences within a series were arranged in a different random order for each subject with the constraint that identical templates never occurred in successive trials. Subjects were free to choose idiosyncratically the tempo with which movements were executed. For template T_2 the tempo was suggested by the experimenter. Subjects were instructed to synchronize the completion of a full movement cycle with the beat of a metronome. The metronome was stopped before the beginning of the recording in order to prevent voluntary corrective actions by the subjects in case of phase slippage. Three periods were tested (d_{T1} = 2.0, d_{T2} = 2.5, and d_{T3} = 3.0 s), and each was repeated three times; the range of d_T values was broad enough to test the effect of rhythm, and yet compatible with smooth, consistent performance. The sequence of trials was again randomized for each subject with the constraint that the same period never occurred in successive trials. In summary, the database consisted of 3 (subjects) × 3 (trajectories) × 3 (modalities; size ratio for T_1 and T_3, period for T_2) × 3 (repetitions) = 81 recordings.

Data Analysis

In all conditions tested the 10-s recording period was sufficient for tracing the curves several times. The left panels in Figure 3 show examples of complete recordings for each template. Position (X, Y), velocity (V_x, V_y), and acceleration (A_x, A_y) components at the three landmarks of the curves (Q_1, Q_2, Q_3), which are needed to derive the minimum-jerk predictions, were measured for each movement cycle. Whenever necessary, indices (e.g., A_{x1}, V_{y3}) will be used to identify the kinematic quantities corresponding to each landmark. The position of the landmarks on the actual trajectories was determined as follows. After moving the center of gravity of the traces to the origin of the reference axes, we computed first and second derivatives of the position components using the optimal FIR (filtering and differentiating) algorithm (Rabiner & Gold, 1975; cutoff frequency: 20 Hz). Then, we applied the following numerical criteria. For T_1, Q_1 and Q_3 are the points where the horizontal velocity component V_x changes sign; Q_2 is the point where curvature changes sign. There are two such points in each cycle but, for our purposes, they were considered as equivalent. For T_2 (upper right lobe), Q_1 (Q_3) is the point where the horizontal (vertical) component of the acceleration becomes negative (positive), and the distance from the center of the coordinate axes is less than ¼ of the average maximum. Q_2 is the point where the distance from the center is maximum. Because T_2 has a fourfold symmetry, there are four sets of equivalent landmarks in each cycle. They were all referred to the upper right lobe. For T_3, Q_1 and Q_3 are the points where the horizontal velocity V_x changes from positive to negative; the two points were discriminated by a criterion on the distance from the center of gravity; Q_2 is the point where the horizontal velocity changes from negative to positive (again, two points of the trajectory satisfy this criterion, but, as for T_1, they were considered as equivalent). The landmarks identified by applying this procedure to all movement cycles in the examples of Figure 3 are indicated by circles superimposed to the traces.

Results

Geometrical Aspects of the Performance

As illustrated by the three typical examples on the left side of Figure 3, subjects had no difficulty tracing the required trajectories with smooth, continuous movements. The examples are also indicative of the relatively small variability of the traces from cycle to cycle. Accuracy and consistency of successive cycles of movement were estimated by computing averages and standard deviations (over cycles, repetitions, and subjects) of the coordinates of the landmarks identified on the recorded traces (Table 1). The results show that both absolute and relative sizes of the templates were reproduced faithfully in all conditions tested. Despite the pooling over subjects and repetitions, the variability of the position of the landmarks was quite small (of the order of 0.5 cm).

Temporal Aspects of the Performance

Although the experimenters did not impose temporal constraints for the execution of T_1 and T_3, subjects spontaneously chose comparable rhythms for the three versions of these templates. The average velocities over movement cycles for T_1 (all model curves had the same perimeter) were S_1 = 33.08 cm/s; S_2 = 34.41 cm/s; S_3 = 33.26 cm/s. The corresponding values for T_3 were: T_{31}: S_1 = 44.94 cm/s; S_2 = 43.81 cm/s; S_3 = 46.84 cm/s; T_{32}: S_1 = 39.54 cm/s; S_2 = 40.78 cm/s; S_3 = 40.78; T_{33}: S_1 = 35.33 cm/s; S_2 = 36.30 cm/s; S_3 = 37.34 cm/s. These results provide further confirmation of the isochrony principle described above: in all subjects the reduction in total perimeter between T_{31} and T_{33} (75 cm vs. 60 cm) spontaneously induced a comparable reduction of the average velocity so that cycle duration remained almost constant. The principle also applies within each movement cycle. Whenever the two parts of T_1 and T_3 had unequal perimeters, the ratio $r_d = d_1/d_2$ between the duration of the two parts was far smaller than the corresponding perimeter ratio r (Table 2). To compare the degree of within-cycle isochrony across conditions, we defined the isochrony coefficient $I = (r - r_d)/(r - 1)$ which takes into account the perimeter ratio (P_1/P_2) and may range between 0 (no velocity compensation) and 1 (perfect isochrony). Although the value of I was significantly less than 1 (pooling over subjects, ratio r and templates, the .99 confidence interval for I was $(0.672 \leq I_m \leq 0.791)$, the corresponding average I_m = 0.732 indicates a strong tendency toward within-cycle isochrony; such a value implies, for instance, that a perimeter ratio r = 5 results in a duration ratio of only about 2.

Subjects modulated the rhythm of execution for template T_2 as indicated by the experimenter. The duration of the cycles was slightly but systematically shorter than the required one (average of d_T across trials and subjects: T_{21} = 1.938 s; T_{22} = 2.314 s; T_{23} = 2.886 s). However, differences among the durations of the four symmetric parts

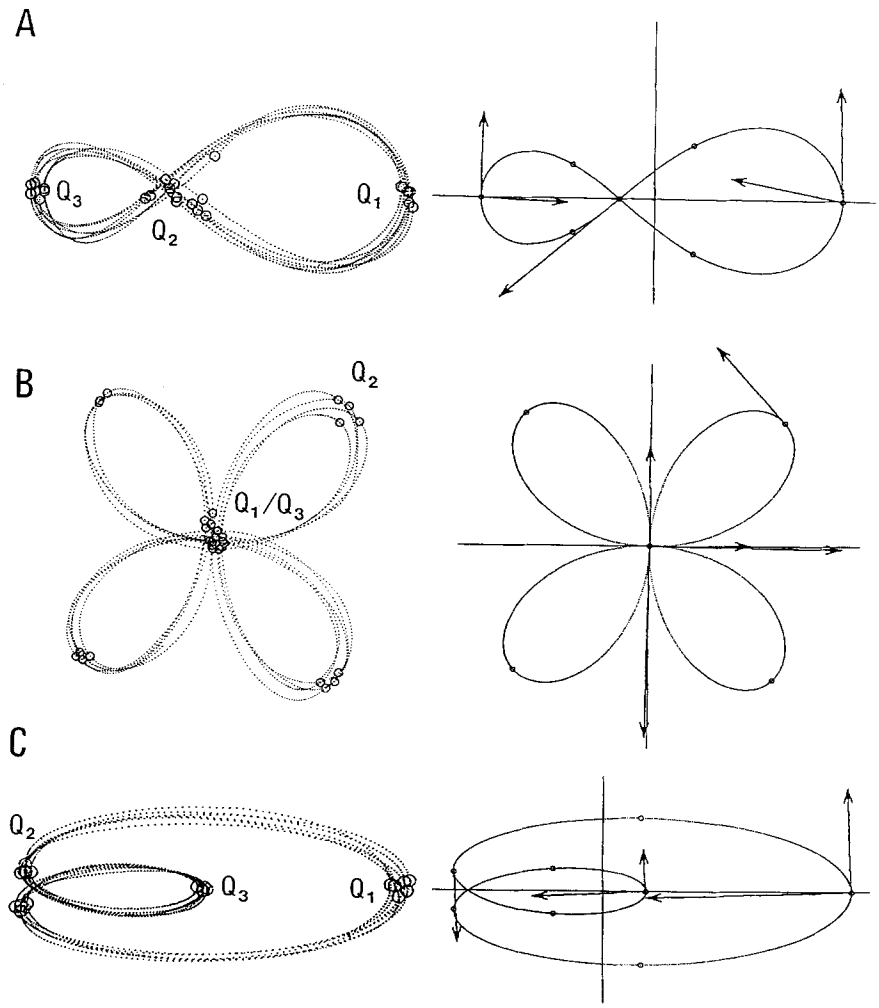

Figure 3. Comparison between actual and simulated trajectories. Patterns on the left are representative examples of continuous tracing movements; each presents data from a different subject for each pattern type. The total duration of the trial was 10 s, and the sampling frequency was 200 samples/s. Landmarks that were used for the quantitative analysis of the performance (circles superimposed on the traces) were located automatically on the basis of kinematic and geometrical criteria (see text for details). Patterns on the right represent trajectories predicted by the minimum-jerk model for the specific trials shown on the left. Boundary conditions (vectors) and total durations for the simulations were computed by averaging the corresponding experimental values over all available cycles in the trial. The symmetries of the templates were forced onto the simulations. Circles indicate landmarks and extrema of curvature.

of this curve were quite small and unsystematic. Fluctuations of the rhythm within trials were also small and nonsignificant.

Relation Between Geometry and Kinematics

The validity of the two-thirds power law was tested separately for each trial. At a qualitative level, this was done by plotting in a doubly logarithmic scale the tangential velocity $V(s)$ versus the quantity $R(s)^* = R(s)/[1 + \alpha R(s)]$. On the basis of previous results (Viviani & Stucchi, 1992) the parameter α was set in all cases to 0.05. According to Equation 1, if the velocity gain factor $K(s)$ were a true piecewise constant (see above), the data points would cluster along unconnected parallel segments of straight lines. More realistically, one expects some kind of smooth transition between successive different K values and, consequently, that these straight lines in the ($\log V - \log R^*$) plots be connected by some more complex segments. These predictions were borne out by the results. For templates T_1 and T_3, K was constant throughout most of the two loops that compose the pattern; transitions (variable gain) always occurred in the proximity of landmarks Q_2 (inflections in T_1 and transition between loops in T_3; see Figure 3). No transition was instead visible for template T_2 that was traced with just one value of the velocity gain. These points are

Table 1
X and Y Coordinates of Measured Landmarks for All Templates and Conditions

Landmarks	*M*	*SD*	TV	*M*	*SD*	TV	*M*	*SD*	TV
				Asymmetric lemniscate					
		T_{11}			T_{12}			T_{13}	
X									
Q_1	8.98	0.44	9.15	11.68	0.53	12.39	13.07	0.45	14.01
Q_2	0.00	0.85	0.00	0.00	0.73	0.00	0.00	0.72	0.00
Q_3	−8.77	0.29	−9.15	−6.33	0.38	−5.87	−4.88	0.27	−4.18
Y									
Q_1	0.07	0.31		0.02	0.39		0.03	0.40	
Q_2	−0.80	0.49		0.01	0.60		−0.09	0.60	
Q_3	−0.10	0.40		−0.13	0.37		−0.13	0.32	
				Cloverleaf					
		T_{21}			T_{22}			T_{23}	
X (Q_2)	6.52	0.57	6.79	6.28	0.61	6.79	0.62	0.79	6.79
Y (Q_2)	6.33	0.45	6.79	6.26	0.47	6.79	6.26	0.40	6.79
				Oblate limaçon					
		T_{31}			T_{32}			T_{33}	
X									
Q_1	6.26	0.76	6.63	9.42	0.59	10.04	13.07	0.45	14.01
Q_2	−12.26	0.37	−12.82	−9.47	0.38	−9.56	−6.28	0.33	−6.51
Q_3	0.00	0.44	0.00	0.00	0.40	0.00	0.00	0.34	0.00
Y									
Q_1	0.01	0.39		−0.24	0.29		−0.02	0.38	
Q_2	0.11	0.64		0.17	0.88		0.07	1.09	
Q_3	0.00	0.29		−0.01	0.28		−0.04	0.24	

Note. Means, standard deviations (in centimeters) and theoretical values (TVs) calculated over subjects and repetitions. Zero reference for *X* values was set at the average horizontal coordinate of the intermediate landmarks (Q_2 for T_1; Q_1/Q_3 for T_2; Q_3 for T_3). All theoretical *Y* values for T_1 and T_3 are zero.

illustrated in Figure 7 with the help of a few examples of complete plots for each template.

A quantitative analysis of the two-thirds power law was also performed by computing for each trial the linear regression of log *V* against log *R**. For T_1 and T_3 separate analyses were made for each loop in the trajectories. Transitions phases around the landmark Q_2 were eliminated by the empirical criterion of discarding the first and last one-eighth portion of trajectory preceding and following Q_2. For T_2 only one regression was performed on all available data points. Figure 4 illustrates the results with a representative example for each experimental condition. The slope of the regression lines estimates the exponent β appearing in Equation 1; the intercept estimates the logarithm of the velocity gain *K*. Tables 3, 4, and 5 summarize the results for T_1, T_2, and T_3, respectively. In general, linear regressions described the data points quite accurately (with a few exceptions, correlation coefficients exceeded 0.9). Also, the overall average estimate of the exponent ($\beta = 0.334$) was virtually identical to that measured in previous studies (cf. above). However, β values for both T_1 and T_3 tended to be higher for the small than for the large loop. Velocity gain factors depended on all experimental variables. For T_2, *K* is directly proportional to the actual rhythm of execution (Figure 5A). For the other two templates, the gain within each loop is a power function of the corresponding perimeter. This is illustrated in Figure 5B, which shows that the logarithm of *K* is a linear function of the logarithm of the actual perimeters of the loops (averages over all repetitions). The existence of a relation between velocity gain and perimeter, and the slopes of the regression lines for the (log *K* − log *P*) scatterplots (≈ 0.5) are in excellent agreement with the results of past experiments. As argued in the introductory section and in more detail elsewhere (Viviani, 1986; Viviani & Cenzato, 1985; Viviani & Schneider, 1991), the fact that, within each unit of the trajectory, *K* is an increasing function of the linear extent of the unit provides an explanation for the phenomenon of local isochrony.

Modeling

The minimum-jerk model simultaneously predicts the trajectory and the kinematics of a movement constrained to pass through a via-point. The prediction depends on a set of boundary conditions: one must specify the duration of the movement as well as position, velocity, and acceleration vectors for both initial and terminal points of the movement. As for the via-point, it is possible either to specify only the position or to specify both position and velocity. The second solution, slightly more constraining, was adopted in our

Table 2
Within-Cycle Isochrony for Asymmetric Lemniscate and Oblate Limaçon

Subject and duration	P_1/P_2								
	d	d_1/d_2	I	d	d_1/d_2	I	d	d_1/d_2	I
	Asymmetric lemniscate								
		$r_1 = 1$			$r_2 = 2$			$r_3 = 3$	
S_1									
d_1	0.710			0.821			0.869		
d_2	0.689	1.030	—	0.663	1.238	0.762	0.622	1.397	0.801
d_T	1.397			1.464			1.492		
S_2									
d_1	0.684			0.809			0.848		
d_2	0.674	1.015	—	0.608	1.331	0.669	1.560	1.514	0.743
d_T	1.359			1.417			1.409		
S_3									
d_1	0.720			0.846			0.930		
d_2	0.716	1.006	—	0.566	1.495	0.505	0.553	1.683	0.658
d_T	1.435			1.412			1.483		
	Oblate limaçon								
		$r_1 = 1.5$			$r_2 = 2$			$r_3 = 3$	
S_1									
d_1	0.872			0.932			0.988		
d_2	0.798	1.093	0.814	0.775	1.202	0.798	0.709	1.393	0.803
d_T	1.669			1.707			1.698		
S_2									
d_1	0.913			0.936			0.996		
d_2	0.800	1.141	0.718	0.718	1.304	0.696	0.657	1.516	0.742
d_T	1.712			1.655			1.653		
S_3									
d_1	0.855			0.924			0.941		
d_2	0.746	1.146	0.708	0.748	1.235	0.765	0.669	1.406	0.797
d_T	1.601			1.655			1.607		

Note. The following data are reported for each subject (S) and each ratio between the perimeters of the two parts of the template ($r = P_1/P_2$): the duration of a complete movement cycle (d_T), the duration of each part (d_1, d_2), the ratio between durations (d_1/d_2), and the value of the isochrony coefficient (I) defined in the text. Durations (in seconds) are averages over three repetitions. The coefficient I is indefinite when the two parts of T_1 are equal ($r = 1$). Dashes denote values of I that cannot be computed.

simulations. The mathematical derivation of the predicted trajectories is similar to the one described in Edelman and Flash (1987); the main difference with respect to the procedure followed in that study is the possibility for velocities and accelerations at the initial and terminal points to have nonzero values. Because templates were symmetrical, data and predictions were compared only over part of a complete cycle. For T_1 and T_3 the half trajectory from landmark Q_1 (starting point) to Q_3 (end point) was modeled. For T_2 we considered only one lobe which, again, begins at Q_1 and ends at Q_3. In all three cases landmark Q_2 was the imposed via-point.[3] Notice that there is more than one way of defining the initial and terminal points for the model; in particular, at least in the case of T_1 and T_3, choosing Q_2 both as starting and end point would also be possible, and, actually, would be in keeping with the reasonable hypothesis that the small and large loops in these templates are construed by the control system as units of motor action. Indeed, it was verified that this solution leads to simulated trajectories that are as satisfactory as those presented here. The solution that we adopted, however, has a major advantage: Because the two (half) units are modeled simultaneously, and passage time at the via-point is not provided as a boundary condition, one may assess how the model predicts the relative duration of the units. Obviously, this possibility would be precluded by the alternative solution that requires one independent simulation for each loop. Moreover, although via-point and terminal constraints are dealt with differently from the mathematical point of view, their role in the simulations is somewhat interchangeable.

[3] This is the only adequate procedure for dealing in general with the single via-point case. The solution adopted by Wann et al. (1988), which consisted of linking two piecewise-polynomial periodic functions at 90° phase, is computationally equivalent to our procedure only in the special case of elliptical trajectories, but cannot be extended to more complex curves. An ellipse can be generated easily with the general procedure by placing both initial and final points on one extremum of the ellipse, the via-point at the other extremum, and by computing the boundary conditions from the Lissajous parametric equations of the ellipse.

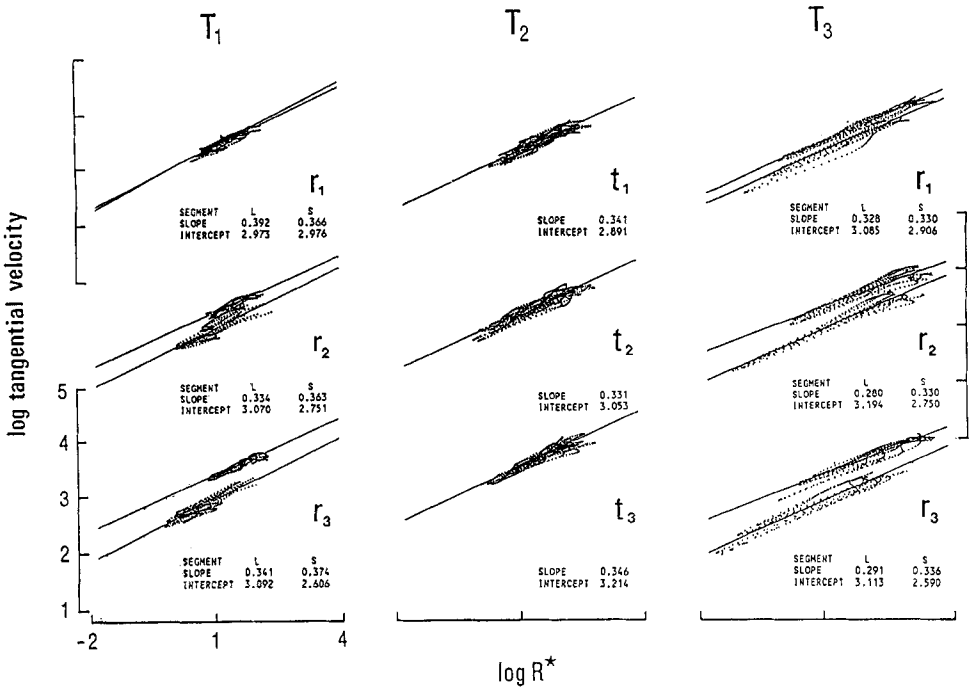

Figure 4. Analysis of the data according to the two-thirds power law. Examples of the scatter diagram that obtains by plotting in doubly logarithmic scales the tangential velocity versus the modified radius of curvature R^*. Each panel corresponds to the indicated modality (size ratio r or cycle duration t) and template type (T). Data for T_1, T_2, and T_3 were obtained from subjects S_1, S_2, and S_3, respectively. For templates T_1 and T_3 the data points close to the transition between small and large loops have been omitted. With the obvious exception of the ($T_1 - r_1$) combination, each loop in these templates gives rise to a clearly identifiable cluster. Linear correlation analysis was performed independently for each cluster. For template T_2 all data points were plotted and analyzed. The slope and the intercept of the regression line estimate the exponent of the law and the logarithm of the velocity gain, respectively. Regression parameters for the examples shown here are given inset.

Minimum-jerk predictions were generated for each trial by using as boundary conditions the kinematic parameters measured from the actual recordings (for Q_1, $[X_1, Y_1]$, $[V_{x1}, V_{y1}]$, $[A_{x1}, A_{y1}]$; for Q_2, $[X_2, Y_2]$, $[V_{x2}, V_{y2}]$, $[A_{x2}, A_{y2}]$; for Q_3, $[X_3, Y_3]$, $[V_{x3}, V_{y3}]$). These values, as well as the total duration of the cycle (a free parameter of the model), were obtained by averaging the corresponding measures for all complete cycles within a trial, and all degrees of symmetry in the template. Appropriate sign changes were applied to the components whenever necessary (e.g., when pooling the components for the two Q_2 landmarks in template T_1).

Qualitative comparisons. The right panels in Figure 3 illustrate with three examples (one trial in one condition for each template) the accuracy with which actual trajectories (left panels) are simulated by the procedure described above. Predicted trajectories were completed by mirror reflection of the portion computed by the model. Velocities and accelerations at the boundaries for these trials are indicated by vectors. Templates were always reproduced as accurately as indicated in these typical examples. Figure 6 extends the comparison to the kinematic aspects of the movement. Each panel in this figure shows an example of model fitting for a different combination of template and condition. The experimental velocity curves for all complete cycles within a trial (dotted lines) are superimposed after normalizing the duration of the cycle. The continuous traces superimposed on the data points are the corresponding predictions of the model. The predictions, which are based on the average boundary conditions over all cycles, faithfully reproduce the main features of the experimental data. Finally, Figure 7—which reports data from the same trials—compares predictions and experimental results concerning the relationship between geometry and kinematics. The rectilinear portions of the scatterplots are clearly present in the simulations. Notice that, unlike the plots of Figure 4, all available data points have been reported here, including those that, in T_1 and T_3, correspond to the transitions between small and large loops. As explained before, the velocity gain factor within these transitions changes rapidly, so that velocity and radius of curvature are no longer related in a simple way. Nonetheless, it is apparent from these typical examples that the minimum-jerk model is able to capture accurately the ($V - R$) relationship even during the transitions.

Quantitative comparisons. The accuracy with which the model predicts the temporal aspects of the performance is

Table 3
Analysis of Individual Data for Asymmetric Lemniscate According to the Two-Thirds Power Law Model

Loop size/ subjects	P_1/P_2 $r_1 = 1$ M	CI	ρ	$r_2 = 2$ M	CI	ρ	$r_3 = 3$ M	CI	ρ
				Exponent β					
Large									
S_1	0.404	±.012		0.328	±.013		0.340	±.011	
S_2	0.289	±.014		0.316	±.011		0.211	±.013	
S_3	0.329	±.014		0.344	±.017		0.294	±.013	
M	0.341			0.329			0.258		
Small									
S_1	0.398	±.013		0.369	±.011		0.381	±.014	
S_2	0.352	±.006		0.316	±.006		0.313	±.008	
S_3	0.387	±.010		0.327	±.011		0.327	±.012	
M	0.379			0.342			0.355		
				Velocity gain factor K (log units)					
Large									
S_1	2.955	±.015	0.917	3.083	±.018	0.876	3.100	±.017	0.903
S_2	3.083	±.014	0.876	3.102	±.017	0.877	3.322	±.022	0.726
S_3	2.951	±.017	0.857	2.991	±.015	0.823	3.089	±.011	0.817
M	2.996		0.883	3.059		0.859	3.170		0.815
Small									
S_1	2.917	±.017	0.917	2.782	±.012	0.903	2.627	±.010	0.903
S_2	3.001	±.014	0.913	2.893	±.010	0.923	2.797	±.009	0.907
S_3	2.922	±.014	0.933	2.877	±.011	0.916	2.782	±.010	0.917
M	2.947		0.921	2.851		0.914	2.735		0.909

Note. The following data are provided for each ratio between small and large loop in the template ($r = P_1/P_2$): the averages over repetitions for subjects S_1, S_2, and S_3, and the 95% confidence intervals (CI) of the exponent β and of the velocity gain factor K. β and K were estimated by linear regression between tangential velocity and radius of curvature in logarithmic scales. ρ = coefficient of correlation for the regression.

illustrated in Table 6. Because the model is time scalable, total movement time is not independent of velocity and acceleration boundary conditions; thus, it is meaningless to compare actual and theoretical durations of a complete movement cycle. By contrast, the passage time at the via-point was not imposed. Thus, for T_1 and T_3, the relative

Table 4
Analysis of Individual Data for Cloverleaf According to the Two-Thirds Power Law Model

Subject	$d_{T1} = 2.0$ M	CI	ρ	$d_{T2} = 2.5$ M	CI	ρ	$d_{T3} = 3.0$ M	CI	ρ
				Exponent β					
S_1	0.368	±.006		0.382	±.005		0.391	±.005	
S_2	0.321	±.005		0.340	±.006		0.348	±.004	
S_3	0.287	±.007		0.338	±.007		0.341	±.005	
M	0.325			0.353			0.360		
				Velocity gain factor K (log units)					
S_1	2.834	±.009	0.945	3.019	±.009	0.957	3.199	±.008	0.967
S_2	2.811	±.010	0.927	3.077	±.009	0.941	3.216	±.008	0.959
S_3	2.933	±.012	0.876	3.042	±.011	0.922	3.189	±.006	0.943
M	2.859		0.916	3.046		0.940	3.201		0.956

Note. The following data are provided for each indicated duration of one cycle (d_T): the averages over repetitions for subjects S_1, S_2, and S_3, and the 95% confidence intervals (CI) of the exponent β and of the velocity gain factor K. β and K were estimated by linear regression between tangential velocity and radius of curvature in logarithmic scales. ρ = coefficient of correlation for the regression.

Table 5
Analysis of Individual Data for Oblate Limaçon According to the Two-Thirds Power Law Model

Loop size/ subject	P_1/P_2								
	$r_1 = 1$			$r_2 = 2$			$r_3 = 3$		
	M	CI	ρ	*M*	CI	ρ	*M*	CI	ρ
	Exponent β								
Large									
S_1	0.329	±.006		0.322	±.008		0.307	±.005	
S_2	0.324	±.007		0.292	±.006		0.284	±.007	
S_3	0.310	±.006		0.283	±.008		0.269	±.006	
M	0.321			0.299			0.287		
Small									
S_1	0.357	±.005		0.372	±.006		0.346	±.007	
S_2	0.324	±.006		0.316	±.006		0.313	±.008	
S_3	0.338	±.008		0.340	±.007		0.342	±.011	
M	0.340			0.343			0.334		
	Velocity gain factor *K* (log units)								
Large									
S_1	3.190	±.016	0.976	3.149	±.013	0.983	3.149	±.014	0.983
S_2	3.239	±.014	0.975	3.248	±.014	0.973	3.260	±.016	0.961
S_3	3.141	±.015	0.969	3.192	±.018	0.956	3.172	±.017	0.951
M	3.190		0.973	3.196		0.971	3.194		0.965
Small									
S_1	2.867	±.009	0.989	2.666	±.011	0.980	2.472	±.011	0.980
S_2	3.078	±.010	0.983	2.907	±.010	0.979	2.704	±.011	0.970
S_3	2.890	±.017	0.966	2.801	±.013	0.980	2.600	±.014	0.962
M	2.945		0.979	2.791		0.981	2.592		0.971

Note. The following data are provided for each ratio between small and large loop in the template ($r = P_1/P_2$): the averages over repetitions for subjects S_1, S_2, and S_3, and the 95% confidence intervals (CI) of the exponent β and of the velocity gain factor *K*. β and *K* were estimated by linear regression between tangential velocity and radius of curvature in logarithmic scales. ρ = coefficient of correlation for the regression.

durations of the two loops and their variations across conditions can be used to test the validity of the model. As demonstrated by the excellent correspondence of the means, and by the high values of the linear correlation coefficients, the model accurately captures the phenomenon of within-cycle isochrony that was illustrated in Table 2 and Figure 5B. No comparison is of course possible for T_2.

Comparison With Two-Thirds Power Law

We investigated how the minimum-jerk model compares with the two-thirds power law in representing the relation between kinematics and curvature. To make the comparison as rigorous as possible, simulated movements were analyzed with the same procedures used to obtain the results of Tables 3 to 5. Specifically, linear regressions between log *V* and log R^* were calculated on comparable segments of trajectories. For T_1 and T_3 we eliminated the same transitions between small and large loops that had been omitted in the plots of Figure 4. For T_2, instead, the entire upper right lobe was included. Moreover, the number of simulated data points used for calculating the linear regressions were made approximately equal to the number of real data points (the real data points are distributed over several cycles of recording; the simulated ones are instead concentrated in just one cycle). Intercepts and slopes of the regression lines through simulated points have the same interpretation as the analogous quantities already computed for the data (i.e., log *K* and β, respectively). Thus, the desired comparison was finally obtained by performing a correlation analysis over 27 pairs of values (3 subjects × 3 conditions × 3 repetitions) for each template. The results are reported in Table 7 (velocity gain factor) and Table 8 (exponent β). As expected on the basis of the good agreement in the time domain, the values of the velocity gain are highly correlated ($r > .9$). The coefficient of linear correlation for the exponent β is not nearly as high, but this is due to the very small range of variability of this parameter across subjects, conditions, and repetitions. Averages are actually quite comparable. Even the small but significant differences between the values of β in the two loops of T_1 and T_3 are captured by the simulated data.

Discussion

We contrasted two ways of studying planar hand movements, each characterized by a different strategy for dealing with the excess degrees of freedom in the hand–arm system. The first strategy attempts to identify certain principles of

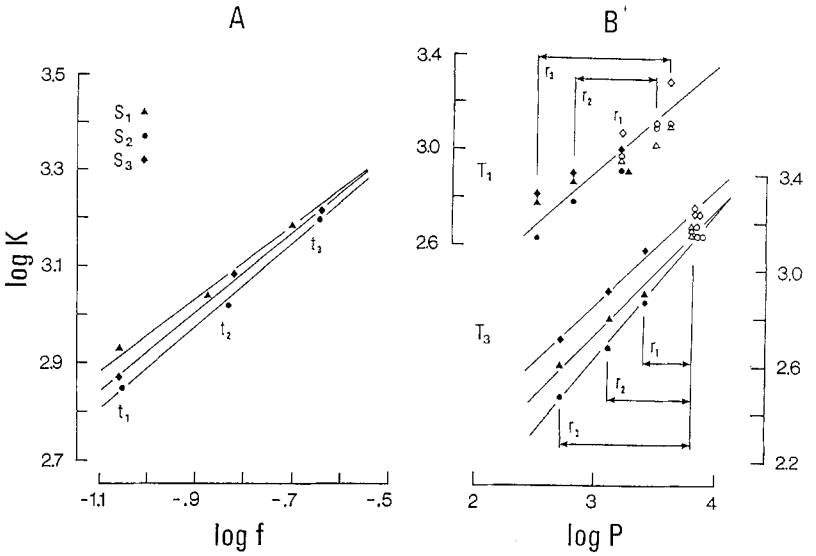

Figure 5. Velocity gain factor and isochrony. Panel A: Results for template T_2. The velocity gain K is plotted in a doubly logarithmic scale as a function of the actual rhythm (f = reciprocal of period) of the movement. Data points are averages over repetitions for each indicated combination of subject and rhythm (t_1, t_2, t_3). Across conditions, K is approximately proportional to the rhythm. A similar tendency can also be found if one considers only the spontaneous variations of rhythm that occur within repetitions. Panel B: Results for templates T_1 and T_3. The velocity gain K within each loop is plotted as a function of the theoretical perimeter P of the loop (log-log scale). Empty and filled symbols are relative to the large and small loops in these templates. Data points are averages over repetitions for each combination of subject and condition. For both templates, the ($P - K$) relationship is adequately described by a power function. The exponent of the relationship (slope of the linear regression through the data points) is comparable in the two cases (T_3 slope for S_1 = 0.501; S_2 = 0.617; S_3 = 0.482; for T_1 only one regression has been calculated: slope = 0.419).

covariation between the trajectory and the kinematics of the movement; the other strategy emphasizes instead the concept of optimal control and leads to an explicit model for movement planning. With the help of a potentially discriminating set of data, we demonstrated an overlap between the solutions that each approach offers to the degrees-of-freedom problem. In what follows we assess the extent of this overlap, as well as the significance of the points of divergence. The analysis of the global pattern of results sets the stage for an attempt to formulate a common framework wherein the two approaches can be reconciled.

In assessing the convergence of our strategies, a distinction has to be made between the two main regularities present in the data. On the one side, the existence of a principled relationship between the form of the trajectory and the velocity of the movement was fully supported by the predictions derived from the minimum-jerk hypothesis. At least in the case of templates T_2 and T_3, an excellent fit to the data points was obtained when each half-movement cycle was characterized as an optimal movement with via-point constraints; the minimum-jerk simulation captured even some subtle details of the (log R^* − log V) plots (see Figure 7) that eluded the formulation of the two-thirds power law in which the gain factor is a true piece-wise constant function. Moreover, the parameters β and K, estimated by fitting the two-thirds power law to both experimental and simulated data, were very similar (see Tables 3 to 5). This agreement extends the conclusions of Wann et al. (1988) to the case of relatively complex trajectories that cannot be generated by single harmonic components. Nevertheless, it is difficult to see how the excellent fit of the velocity curves obtained with a kinematic model (see Figure 6) could be improved by formulating the minimization criterion in terms of dynamic variables, as these authors claimed. The introduction of cost variables such as "wobble" (Wann et al., 1988), torques (Uno et al., 1989), energy (Nelson, 1983), or stiffness (Hasan, 1986) might be motivated by physiological and developmental arguments, but even more complex motor tasks than those studied here will have to be considered before passing a final judgment on the basis of empirical evidence.

As for the phenomenon of isochrony, the comparison between our two approaches is more delicate. The motor program view assumes that the execution stage has access to a representation of the intended gesture which, among other things, includes an estimate of the linear extent of the trajectory. Thus, this view provides an adequate framework for accommodating the finding that average velocity scales with trajectory length. In fact, it was shown (Viviani & Cenzato, 1985) that the case of complex trajectories com-

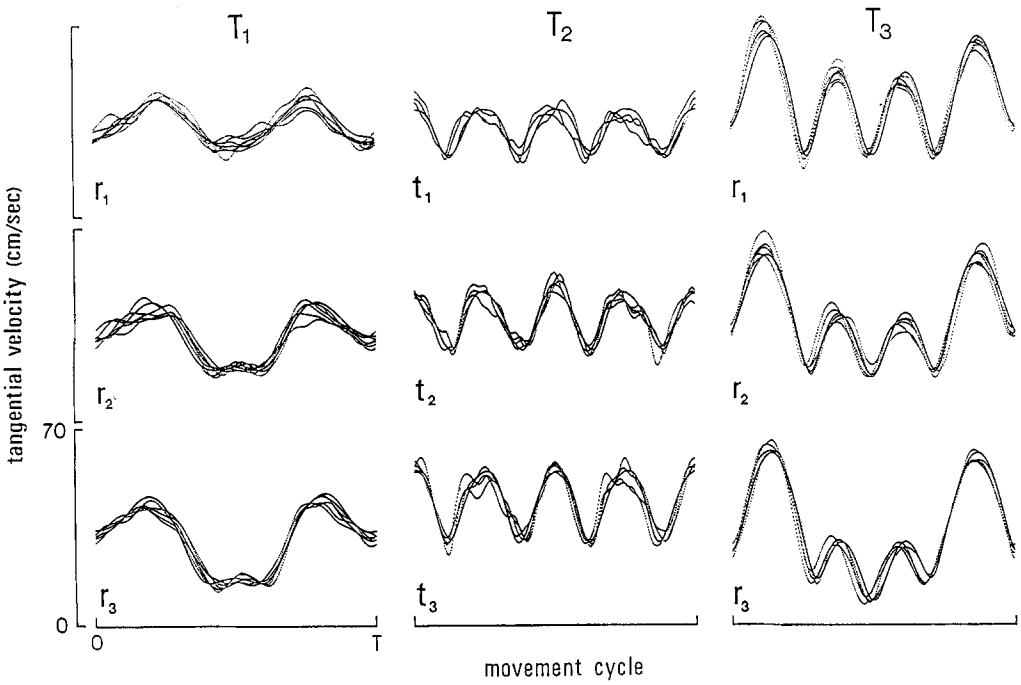

Figure 6. Comparison between actual and simulated velocities. Each panel shows an example relative to the indicated modality (size ratio r or cycle duration t) and template type (T). Data for T_1, T_2, and T_3 were obtained from subjects S_1, S_2, and S_3, respectively. The amplitude of the tangential velocity across all available complete cycles of movement within a trial (represented by the light dotted lines) is compared with the prediction of the minimum-jerk model for the same specific trial (represented by the heavy, continuous lines). Boundary conditions and total durations for these simulations were computed by averaging the corresponding experimental values over all cycles in the trial. To facilitate comparison across experimental modalities, the horizontal (time) scales for both actual and simulated curves were normalized to an arbitrary value. Notice the high cycle-by-cycle stability of the motor performances and the excellent accuracy of the theoretical predictions.

posed of distinct subunits, in which local (within units) and global (across units) velocity scaling interact, also can be handled within this framework. By contrast, in minimum-cost models both the trajectory and the law of motion are specified concurrently by the initial, final, and via-point conditions; the length of the actual trajectory is not supposed to be represented internally. Because total movement time is a free parameter, the phenomenon of global isochrony cannot, even in principle, be deduced within the minimum-jerk model, nor, in fact, within any other cost-minimizing model that does not include movement duration in the cost function. It is interesting, however, that relative isochrony can be predicted and, indeed, the correlation analysis showed that the variations across conditions of the duration of the small and large loops in T_1 and T_3 are accurately reproduced by the model, even though the passage time through the via-point was not imposed.

Experimental and simulated data were analyzed within the conceptual framework provided by the two-thirds power law and isochrony. That fits to the data were satisfactory in both cases proves that this framework is congruent with the hypothesis of optimality. Small but significant differences were present, however. The minimum-jerk model slightly overestimated the longer durations of the small and large loops in T_1 and underestimated the shorter durations (see Table 6). Moreover, for T_1 there was a discrepancy between the estimates of the velocity gain factor obtained directly from the experimental data points and those obtained from the simulated movements (see Table 7). The agreement was far better for T_3, which has no inflection points, suggesting that these discrepancies are at least in part due to the small but inevitable differences between the portion of trajectory taken into account for computing K (recall that segments close to the inflections were discarded both in the actual data and in the simulation). The same reason may also be invoked for the significant difference between the estimates of the exponent β (slope of the [log R^* − log V] relationship) for T_1 and T_3 (see Table 8). However, by fitting the two-thirds power law to the points generated by the minimum-jerk model, one observes a similar difference between the values of β for the small and large loop. Finally, the fact that the velocity gain factor for T_2 covaried with the externally imposed rhythm precisely as predicted (r = .985, slope = .988) indicates that time-scalability of the model is reflected in the relation between curvature and velocity precisely as suggested by the two-thirds power law.

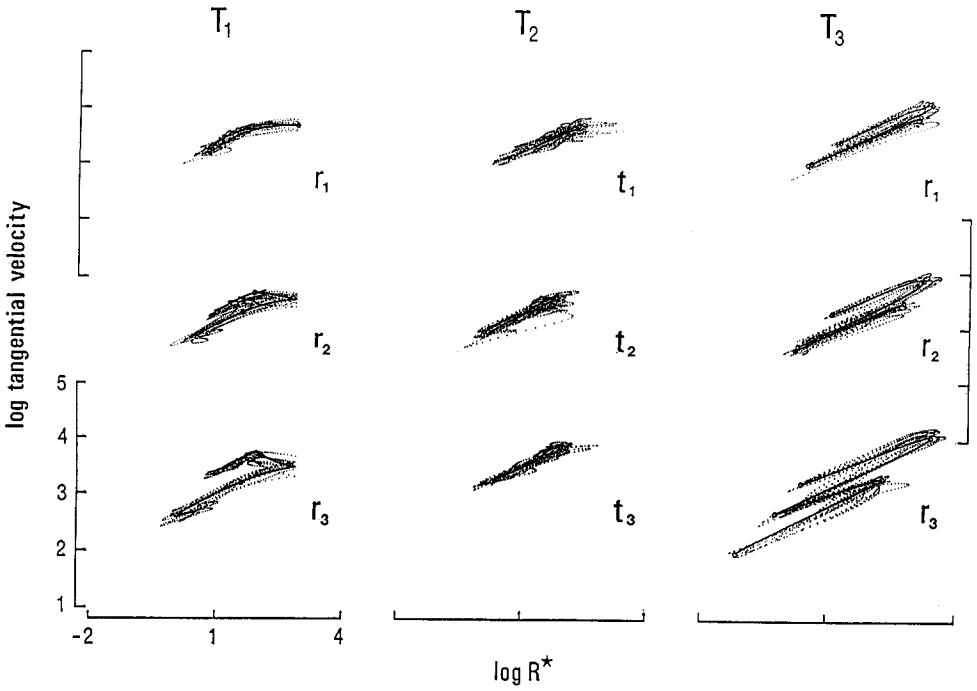

Figure 7. Relation between tangential velocity and modified radius of curvature. (Comparison of data [light dotted lines] and simulation [heavy, continuous lines].) Unlike the similar scatterplots of Figure 4, all available data were included in each panel. Boundary conditions and total durations for the simulations were computed by averaging the corresponding experimental values over all cycles in the trial. Circles superimposed on the heavy lines indicate the points where the curvature of the simulated trajectory attains an extremum. These points delimit the segments of trajectory used to calculate the predicted parameters K and β (see text). Notice that the minimum-jerk model predicts accurately the ($R^* - V$) relationship also during the transitions between loops in T_1 and T_3.

Minimum-cost models are intrinsically more parsimonious than motor programming ones; as such, they ought to be preferred whenever experimental evidence weighs equally on both sides. Given the considerable success with which the minimum-jerk model was able to account for the relationship between velocity and curvature, without making reference to any internal representation of the entire intended trajectory, there is ground to ask whether one should drop all reference to such a hypothetical representation.

We see at least three reasons to resist such an iconoclastic temptation. The first one is that, as we already emphasized before, minimum-cost models deal satisfactorily with relative time structure across movement units, but cannot, by definition, account for global isochrony. One would then be forced to hold a rather contrived hypothesis, namely, that local and global isochrony are generated at different stages of the control process. Also, it would be equally unsatisfactory to imagine that the length of an intended trajectory is available to the control system, as it is necessary to explain global isochrony, whereas the form of the trajectory is not represented in any form.

The second reason for preserving the notion of internally represented trajectory is because it affords a unified framework for dealing with both spontaneous and pursuit tracking movements (Viviani, 1990). It is generally admitted that, in order to reproduce a target movement effectively, we must anticipate certain aspects of its future course. If one assumes, in tune with the general motor programming philosophy, that kinematic details are specified by taking into account the form of the intended trajectory, anticipation in tracking tasks may exclusively concern the future position of the target. The situation is different in minimum-jerk planning where position at any time depends on velocity and acceleration at some future point (via-point or end point). Thus, if tracking movements were planned with this logic, one would expect performance to depend on the ability to predict kinematic variables. Experiments on two-dimensional visuomanual pursuit tracking (Viviani, Campadelli, & Mounoud, 1987; Viviani & Mounoud, 1990) do not support this inference. In fact, it has been shown that the accuracy of tracking performance depends critically on the local relationship between velocity and curvature, and not on future kinematic variables. Indeed, the single most important predictor of the accuracy is whether the target conforms with the two-thirds power law.

Finally, the third reason has to do with recent neurophysiological work by Massey, Lurito, Pellizzer, and Georgopoulos (1992), Schwartz (1992), and Schwartz, Kakavand, and Adams (1991). Massey et al. investigated

Table 6
Comparison Between Experimental (Exp) and Predicted Values of the Duration (in Seconds) of the Two Loops in Template T_1 (Asymmetric Lemniscate) and T_3 (Oblate Limaçon)

Loop size/ duration	Exp	Model	ρ	Slope	A/B
		Asymmetric lemniscate			
Large					
M	0.804	0.793	0.921	1.157	4.978
SD	0.084	0.095			
Small					
M	0.626	0.637	0.866	1.249	3.812
SD	0.063	0.071			
		Oblate limaçon			
Large					
M	0.929	0.936	0.980	0.985	9.928
SD	0.055	0.045			
Small					
M	0.735	0.728	0.979	0.938	9.797
SD	0.056	0.050			

Note. Linear correlation coefficient (ρ), slope of normal regression, and ratio between major and minor axes of the confidence ellipse (A/B) were calculated over 3 (subjects) × 3 (conditions) × 3 (repetitions) = 27 pairs of values. Experimental values are averages over all complete cycles within a trial.

virtual three-dimensional trajectories produced by applying forces to an isometric manipulandum. In their experiments the components of the force along the sagittal, vertical, and lateral axes were transformed into the coordinates of a light point which, with the help of suitable stereo-imaging techniques, appeared to the subject as moving in frontal space. In one task, subjects had to generate forces that corresponded visually to a dynamic three-dimensional scribble. The coordinates of these displays can be manipulated exactly as the coordinates of real movements; in particular, one can compute the velocity of the point, the radius of curvature of the virtual trajectory (within the osculating plane), and investigate their mutual relationship. It was found that the two-thirds power law applies to these virtual movements with the same degree of accuracy observed for real planar scribbles. Thus, whereas nothing in the isometric forces corresponds directly to either velocity or curvature, strength and timing of the motor commands are constrained in a way that is well described by the power law. Moreover, because the power law has been found to be congruent with the hypothesis of optimal control, one can surmise that the latter applies also to the isometric efforts investigated by Massey et al.

Equally relevant are the results of Schwartz (1992), who recorded the activity of single neurons in the primary motor cortex of monkeys performing a visuomanual tracking task. By analyzing the neural population vectors according to the method pioneered by Georgopoulos and collaborators (Georgopoulos et al., 1982), he was able to show that an accurate representation of the kinematic parameters related to arm's trajectory is shown in the discharge patterns of motor cortical cells. Moreover, the discharge components that relate to curvature and velocity are inversely related in this internal representation, as suggested by the two-thirds power law.

Taken together, these results strongly suggest that the covariation between curvature and velocity corresponds to functional principles that pertain to the motor control stage where commands are planned; at the same time, they are incompatible with the alternative interpretation of the covariation as an epiphenomenon of the movement execution stage. Because similar regularities exist both in the force field and in the displacement, it appears as though the second-order dynamic transformation that turns forces into movement does not destroy the relationship described by the two-thirds power law. Because of the convergence between minimum-jerk and power law formalisms, it may be supposed that, to the extent that the minimum-jerk model is successful in predicting kinematic quantities, it might be equally successful in predicting the evolution of the force variables that are responsible for the movement. We return momentarily to the possible significance of this observation.

To conclude, we suggest, in broad qualitative terms, a framework for encompassing both the optimal control and the motor program approaches. The argument is based on the notion of virtual equilibrium trajectory introduced by Feldman (1974) and elaborated further by a number of authors (Bizzi, Accornero, Chapple, & Hogan, 1982; Feldman, 1986; Flash, 1987, 1989; Hogan, 1984) in an

Table 7
Comparison Between Experimental (Exp) and Predicted Values of the Velocity Gain Factor for the Two Loops in Template T_1 (Asymmetric Lemniscate) and T_3 (Oblate Limaçon) and for the Entire Lobe in Pattern T_2 (Cloverleaf)

Loop size/ lobe/duration	Exp	Model	ρ	Slope	A/B
		Asymmetric lemniscate			
Large loop					
M	21.81	20.71	0.901	0.943	4.397
SD	2.69	2.55			
Small loop					
M	17.30	16.61	0.938	1.080	5.601
SD	1.89	2.04			
		Cloverleaf			
Lobe					
M	21.15	19.93	0.985	0.988	11.597
SD	2.85	2.82			
		Oblate limaçon			
Large loop					
M	24.42	24.21	0.935	0.994	5.471
SD	1.55	1.54			
Small loop					
M	16.31	16.49	0.995	0.965	19.648
SD	2.86	2.76			

Note. Linear correlation coefficient (ρ), slope of normal regression, and ratio between major and minor axes of the confidence ellipse (A/B) were calculated over 3 (subjects) × 3 (conditions) × 3 (repetitions) = 27 pairs of values. Experimental values are averages over all complete cycles within a trial.

Table 8
Comparison Between Experimental (Exp) and Predicted Values of the Exponent β for Two Loops in Template T_1 (Asymmetric Lemniscate) and T_3 (Oblate Limaçon) and for the Entire Lobe in Pattern T_2 (Cloverleaf)

Loop size/ lobe/duration	Exp	Model	ρ	Slope	A/B
		Asymmetric lemniscate			
Large loop					
M	0.317	0.369	0.753	1.281	2.724
SD	0.054	0.063			
Small loop					
M	0.359	0.419	0.270	1.024	1.319
SD	0.030	0.032			
		Cloverleaf			
Lobe					
M	0.346	0.385	0.833	0.525	3.912
SD	0.038	0.026			
		Oblate limaçon			
Large loop					
M	0.302	0.305	0.255	0.168	2.094
SD	0.045	0.027			
Small loop					
M	0.341	0.343	0.772	0.875	2.805
SD	0.035	0.045			

Note. Linear correlation coefficient (ρ), slope of normal regression, and ratio between major and minor axes of the confidence ellipse (A/B) were calculated over 3 (subjects) × 3 (conditions) × 3 (repetitions) = 27 pairs of values. Experimental values are averages over all complete cycles within a trial.

attempt to allay certain problems of the mass-spring model. Briefly, the idea put forward by these authors was that the equilibrium point, which, in the mass-spring model controls muscular synergies, is not abruptly shifted from the initial to the final position, as in earlier versions of the model, but evolves continuously along a centrally represented, virtual trajectory. The gist of our proposal (cf. Flash, 1989, 1990), then, is to assume that what is generated according to the minimum-jerk model is not movement itself, as suggested initially (Flash & Hogan, 1985; Hogan, 1984), but the virtual trajectory that drives the movement in the mass-spring scheme (Figure 8). Therefore, according to our hypothesis, the congruence between experimental data and the predictions of the model would simply reflect its adequacy in representing the evolution of the virtual trajectory.

In order for this proposal to work certain conditions should be met. First, the dynamic properties of neuromuscular transduction must preserve minimum-jerk optimality; in other words, optimal virtual trajectories must map into optimal real movements (the cost function possibly being different). Second, in order to account for the neurophysiological findings mentioned above, it must also be assumed that, when movement is impeded, the relational properties of the virtual trajectory map isomorphically into analogous properties of the isometric force field. Third, the scheme of Figure 8 should be able to deal with the hypothesis that complex trajectories are generated by chaining smaller units of motor action.

We can offer no experimental evidence that these conditions are fulfilled. Plausible arguments can, however, be advanced. As for the first point, one notes that neuromuscular transduction is generally approximated by second-order differential equations (e.g., Equation 7 in Hogan, 1984; Equation 2 in Flash, 1987). From the functional point of view, this amounts to describing movement as a "smoothed" (low-pass filtered) version of the driving motor command. It is then reasonable to suppose that a minimum cost criterion that is based on smoothness may survive the effect of such transduction. As for the correspondence between virtual trajectory and isometric force field, it cannot be a simple one because, with the exception of a few special situations, forces and displacements are not collinear. However, the relational properties that we are considering involve exclusively differential quantities. As such, they ought to be more robust than those involving absolute quantities.

Finally, concerning the chunking of movement into units of motor action, the most important question is the manner in which the motor system may (a) maintain the correct order of the units, and (b) assure smooth continuity at the transition between units. The first requirement applies to all models of motor behavior. As far as we see, in the case of complex, learned sequences of units, it can only be satisfied by resorting to the same conceptual device postulated by

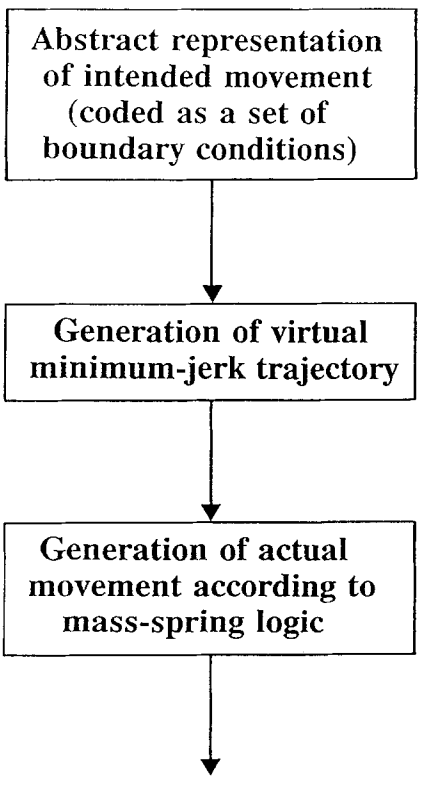

Figure 8. Block diagram illustrating the conceptual relationship among the hypothetical principles involved in the planning of the movement.

Lashley (1951) more than 40 years ago, namely a pointer that scans a preset sequential table. The smooth continuity condition is satisfied by the minimum-jerk model almost by definition. In fact, the chaining of the units in the model is obtained by identifying the end point of a segment with the initial point of the next one, and by equating the corresponding boundary conditions on velocities and accelerations. This ensures continuity of the derivatives; moreover, it provides a straightforward way of accounting for the coupling between adjacent units, that is, for the experimental observation that velocity gain factors of adjacent units are not independent (Viviani & Cenzato, 1985).

The proposal outlined above compounds some interesting features of both the cost-minimization and motor program views. It retains the core notion that motor planning conforms to a principle of optimization, and, at the same time, also the notion that the plan is represented internally prior to its implementation. The covariations between geometry and kinematics may well be emergent properties of the optimum principle, but, by virtue of being properties of a centrally represented plan, and not merely of the actual movement, they may possess a functional role. In particular, the factorization of the instantaneous velocity into a gain factor K and a form-dependent term R^* (Equation 1) may capture the intrinsic time-scalability of many hand movements, and account for the fact that, in many cases, temporal scaling is approximately ratiomorphic. At the same time, our proposal also accommodates within a unified framework the phenomenon of global isochrony that the minimum-jerk model cannot account for (see above). In fact, to the extent that virtual trajectories are construed as internal blueprints, they may carry the metric information on trajectory length that is necessary for global isochrony to exist. Finally, our proposal does not contradict the spirit of recent attempts to model the learning of point-to-point movements within the framework of supervised neural networks (Jordan, Flash, & Arnon, in press). In fact, it has been shown that these models are intrinsically congruent with the criterion of maximum smoothness that is at the basis of the minimum-jerk model. We must acknowledge, however, that the scheme outlined in Figure 8 makes no provision for dealing with motor planning in pursuit tracking tasks, and therefore does not solve the difficulty mentioned before.

In conclusion, the picture emerging from our comparison between strategies for studying movement planning confirms and extends the observation by Flash and Hogan (1985) and Wann et al. (1988) that velocity-curvature covariations are implicit in the minimum-jerk hypothesis. However, the fact that our motor tasks were much more complex than those considered previously, and that the analysis was more thorough and quantitative, led us to somewhat different conclusions. In particular, we do not believe that either one of the two approaches discussed in this article should be abandoned in favor of the other. Pending future research, these approaches, and the conceptual background to which they refer, appear to be compatible and, indeed, integrable into a unified framework.

References

Alexander, G. E., & Crutcher, M. D. (1990a). Neural representations of target (goal) of visually guided arm movements in three motor areas of the monkey. *Journal of Neurophysiology, 64,* 164–178.

Alexander, G. E., & Crutcher, M. D. (1990b). Preparation for movement: Neural representations of intended direction in three motor areas of the monkey. *Journal of Neurophysiology, 64,* 133–150.

Binet, A., & Courtier, J. (1893). Sur la vitesse des gestes graphiques [On the speed of voluntary movements]. *Revue Philosophique, 35,* 664–671.

Bizzi, E., Accornero, N., Chapple, W., & Hogan, N. (1982). Arm trajectory formation in monkeys. *Experimental Brain Research, 46,* 139–143.

Bryson, A. E., & Ho, Y. C. (1975). *Applied optimal control.* New York: Hempshire.

Crutcher, M. D., & Alexander, G. E. (1990). Movement-related neuronal activity selectively coding either direction or muscle pattern in three motor areas of the monkey. *Journal of Neurophysiology, 64,* 151–163.

Derwort, A. (1938). Untersuchungen über den Zeitablauf figurierter Bewegungen beim Menchen [Investigations on the time course of tracing movements]. *Pflügers Archiv für die Gesamte Physiologie des Menschen und der Tiere, 240,* 661–675.

Edelman, S., & Flash, T. (1987). A model of handwriting. *Biological Cybernetics, 57,* 25–36.

Ellis, A. W. (1988). Modeling the writing process. In G. Denes, C. Semenza, P. Bisiacchi, & E. Andreewski (Eds.), *Perspectives in cognitive neuropsychology* (pp. 199–211). Hillsdale, NJ: Erlbaum.

Feldman, A. G. (1974). Change of muscle length due to shift of the equilibrium point of the muscle-load system. *Biofizika, 19,* 534–538.

Feldman, A. G. (1986). Once more on the equilibrium-point hypothesis (Lambda model) for motor control. *Journal of Motor Behavior, 18,* 17–54.

Fitts, P. M. (1954). The information capacity of the human motor system in controlling the amplitude of movement. *Journal of Experimental Psychology, 47,* 381–391.

Flash, T. (1987). The control of hand equilibrium trajectories in multi-joint arm movements. *Biological Cybernetics, 57,* 257–274.

Flash, T. (1989). Generation of reaching movements: Plausibility and implications of the equilibrium trajectory hypothesis. *Brain, Behavior and Evolution, 33,* 63–68.

Flash, T. (1990). The organization of human arm trajectory control. In J. Winters & S. Woo (Eds.), *Multiple muscle systems: Biomechanics and movement organization* (pp. 282–301). Berlin: Springer Verlag.

Flash, T., & Hogan, N. (1985). The coordination of arm movements: An experimentally confirmed mathematical model. *Journal of Neuroscience, 5,* 1688–1703.

Freeman, F. N. (1914). Experimental analysis of the writing movement. *Psychological Review Monograph Supplement, 17,* 1–46.

Georgopoulos, A. P., Kalaska, J. F., Caminiti, R., & Massey, J. T. (1982). On the relations between the direction of two-dimensional movements and cell discharge in primate motor cortex. *Journal of Neuroscience, 2,* 1527–1537.

Georgopoulos, A. P., Kettner, R. E., & Schwartz, A. B. (1988). Primate motor cortex and free arm movements to visual targets

in three-dimensional space: II. Coding the direction by a neuronal population. *Journal of Neuroscience, 8,* 2928–2937.

Guggenheimer, W. H. (1963). *Differential geometry.* New York: Dover.

Haken, H., & Wunderlin, A. (1990). Synergetics and its paradigm of self-organization in biological systems. In H. T. A. Whiting, O. G. Meijer, & P. C. W. van Wieringen (Eds.), *The natural–physical approach to movement control* (pp. 1–36). Amsterdam: VU University Press.

Hasan, Z. (1986). Optimized movement trajectories and joint stiffness in unperturbed, inertially loaded movements. *Biological Cybernetics, 53,* 373–382.

Hogan, N. (1984). An organizing principle for a class of voluntary movements. *Journal of Neuroscience, 4,* 2745–2754.

Hogan, N., & Flash, T. (1987). Moving gracefully: Quantitative theories of motor coordination. *Trends in Neuroscience, 10,* 170–174.

Hollerbach, J. M. (1977). The minimum energy movement for a spring muscle model. *MIT Artificial Intelligence Laboratory Memo 424,* 1–28.

Hollerbach, J. M. (1981). An oscillatory theory of handwriting. *Biological Cybernetics, 39,* 139–156.

Jack, W. R. (1895). On the analysis of voluntary muscular movements by certain new instruments. *Journal of Anatomy and Physiology, 29,* 473–478.

Jordan, M. I. (1990). Motor learning and the degrees of freedom problem. In M. Jeannerod (Ed.), *Attention and performance* (Vol. 13, pp. 796–836). Hillsdale, NJ: Erlbaum.

Jordan, M. I., Flash, T., & Arnon, Y. (in press). A model of the learning of arm trajectories from spatial deviations. *Journal of Cognitive Neuroscience.*

Kalaska, J. F., Cohen, D. A. D., Hyde, M. L., & Prud'homme, M. (1989). A comparison of movement direction-related versus load direction-related activity in primary motor cortex, using a two-dimensional reaching task. *Journal of Neuroscience, 9,* 2080–2102.

Kalaska, J. F., Cohen, D. A. D., Prud'homme, M., & Hyde, M. L. (1990). Parietal area 5 neuronal activity encodes movement kinematics, not movement dynamics. *Experimental Brain Research, 80,* 351–364.

Kay, B. A. (1988). The dimensionality of movement trajectories and the degree of freedom problem: A tutorial. *Human Movement Science, 7,* 343–364.

Keele, S. W. (1981). Behavioral analysis of movement. In V. B. Brooks (Ed.), *Handbook of physiology: Vol. 2. Motor control, Part 2* (pp. 1391–1414). Baltimore, MD: American Physiological Society.

Kelso, J. A. S. (1981). On the oscillatory basis of movement. *Bulletin of the Psychonomic Society, 18,* 63.

Kelso, J. A. S., & Schöner, G. (1987). Toward a physical (synergetic) theory of biological coordination. *Springer Proceedings in Physics, 19,* 224–237.

Kelso, J. A. S., Schöner, G., Scholz, J. P., & Haken, H. (1987). Phase-locked modes, phase transitions and components oscillators in biological motion. *Physica Scripta, 35,* 79–87.

Lacquaniti, F., & Soechting, J. F. (1982). Coordination of arm and wrist movements during a reaching task. *Journal of Neuroscience, 2,* 399–408.

Lacquaniti, F., Terzuolo, C. A., & Viviani, P. (1983). The law relating kinematic and figural aspects of drawing movements. *Acta Psychologica, 54,* 115–130.

Lacquaniti, F., Terzuolo, C. A., & Viviani, P. (1984). Global metric properties and preparatory processes in drawing movements. In S. Kornblum & J. Requin (Eds.), *Preparatory states and processes* (pp. 357–370). Hillsdale, NJ: Erlbaum.

Lashley, K. S. (1951). The problem of serial order in behavior. In L. A. Jeffress (Ed.), *Cerebral mechanisms in behavior. The Hixon symposium* (pp. 112–136). New York: Wiley.

Massey, J. T., Lurito, J. T., Pellizzer, G., & Georgopoulos, A. P. (1992). Three-dimensional drawings in isometric conditions: Relation between geometry and kinematics. *Experimental Brain Research, 88,* 685–690.

Morasso, P. (1981). Spatial control of arm movements. *Experimental Brain Research, 42,* 223–227.

Nagasaki, H. (1989). Asymmetry velocity and acceleration profiles of human arm movements. *Experimental Brain Research, 74,* 319–326.

Nelson, W. L. (1983). Physical principles for economies of skilled movements. *Biological Cybernetics, 46,* 135–147.

Rabiner, L. R., & Gold, B. (1975). *Theory and application of digital signal processing.* Englewood Cliffs, NJ: Prentice Hall.

Rosenbaum, D., Vaughan, J., Jorgensen, M. J., Barnes, H. J., & Stewart, E. (1993). Plans for object manipulation. In D. Meyer & S. Kornblum (Eds.), *Attention and performance* (Vol. 14, pp. 803–820). Hillsdale, NJ: Erlbaum.

Saltzman, E. L., & Kelso, J. A. S. (1987). Skilled actions: A task dynamic approach. *Psychological Review, 94,* 84–106.

Schmidt, R. A. (1975). A schema theory of discrete motor skill learning. *Psychological Review, 82,* 225–260.

Schmidt, R. A. (1976). The schema as a solution to some persistent problems in motor learning theory. In G. E. Stelmach (Ed.), *Motor control: Issues and trends* (pp. 41–65). San Diego, CA: Academic Press.

Schmidt, R. A. (1987). *Motor control and learning.* Champaign, IL: Human Kinetics.

Schneider, R. (1987). *Le concept d'unité d'action motrice et son rôle dans l'organisation spatio-temporelle des gestes graphiques* [The concept of unit of motor action and its role in the spatio–temporal organization of graphomotricity]. Unpublished doctoral dissertation, University of Geneva, Switzerland.

Schöner, G. (1990). A dynamic theory of coordination of discrete movements. *Biological Cybernetics, 63,* 257–270.

Schöner, G., & Kelso, J. A. S. (1988). Dynamic pattern generation in behavioral and neural systems. *Science, 239,* 1513–1520.

Schwartz, A. B. (1992). Motor cortical activity during drawing movements: Single-unit activity during sinusoidal tracing. *Journal of Neurophysiology, 68,* 528–541.

Schwartz, A. B., Kakavand, A., & Adams, J. L. (1991). Behavioral invariants encoded in motor cortical activity. *Society for Neuroscience Abstracts, 2,* 375.

Soechting, J. F., & Lacquaniti, F. (1981). Invariant characteristics of a pointing movement in man. *Journal of Neuroscience, 1,* 710–720.

Soechting, J. F., Lacquaniti, F., & Terzuolo, C. (1986). Coordination of arm movements in three-dimensional space: Sensorimotor mapping during drawing movements. *Neuroscience, 17,* 295–311.

Stelmach, G. E., Mullins, P. A., & Teulings, H. L. (1984). Motor programming and temporal patterns in handwriting. *Annals of the New York Academy of Science, 423,* 144–157.

Teulings, H. L., Mullins, P. A., & Stelmach, G. E. (1986). The elementary units of programming in handwriting. In H. R. S. Kao, G. P. Van Galen, & R. Hoosain (Eds.), *Graphonomics: Contemporary research in handwriting* (pp. 21–32). Amsterdam: North-Holland.

Uno, Y., Kawato, M., & Suzuki, R. (1989). Formation and control

of optimal trajectory in human multijoint arm movement. *Biological Cybernetics, 61,* 89–101.

Van Galen, G. P. (1991). Handwriting: Issues for psychomotor theory. *Human Movement Science, 10,* 165–191.

Viviani, P. (1986). Do units of motor action really exist? In H. Heuer & C. Fromm (Eds.), *Generation and modulation of action patterns* (pp. 201–216). Berlin: Springer-Verlag.

Viviani, P. (1990). Common factors in the control of free and constrained movements. In M. Jeannerod (Ed.), *Attention and performance* (Vol. 13, pp. 345–373). Hillsdale, NJ: Erlbaum.

Viviani, P., Campadelli, P., & Mounoud, P. (1987). Visuo–manual pursuit tracking of human two-dimensional movements. *Journal of Experimental Psychology: Human Perception and Performance, 13,* 62–78.

Viviani, P., & Cenzato, M. (1985). Segmentation and coupling in complex movements. *Journal of Experimental Psychology: Human Perception and Performance, 11,* 828–845.

Viviani, P., & McCollum, G. (1983). The relation between linear extent and velocity in drawing movements. *Neuroscience, 10,* 211–218.

Viviani, P., & Mounoud, P. (1990). Perceptuo–motor compatibility in pursuit tracking of two-dimensional movements. *Journal of Motor Behavior, 22,* 407–443.

Viviani, P., & Schneider, R. (1991). A developmental study of the relation between geometry and kinematics in drawing movements. *Journal of Experimental Psychology: Human Perception and Performance, 17,* 198–218.

Viviani, P., & Stucchi, N. (1992). Biological movements look constant: Evidence of motor perceptual interactions. *Journal of Experimental Psychology: Human Perception and Performance, 18,* 603–623.

Viviani, P., & Terzuolo, C. A. (1980). Space-time invariance in learned motor patterns. In G. A. Stelmach & J. Requin (Eds.), *Tutorials in motor behavior* (pp. 525–533). Amsterdam: North-Holland.

Viviani, P., & Terzuolo, C. A. (1982). Trajectory determines movement dynamics. *Neuroscience, 7,* 431–437.

Wann, J., Nimmo-Smith, I., & Wing, A. M. (1988). Relation between velocity and curvature in movement: Equivalence and divergence between a power law and a minimum-jerk model. *Journal of Experimental Psychology: Human Perception and Performance, 14,* 622–637.

Whiting, H. T. A. (1984). *Human motor actions: Bernstein revisited.* Amsterdam: Elsevier.

Wing, A. M. (1978). Response timing in handwriting. In G. E. Stelmach (Ed.), *Information processing in motor control and learning* (pp. 153–172). San Diego, CA: Academic Press.

Wing, A. M. (1979). Variability in handwritten characters. *Visible Language, 13,* 283–298.

Wing, A. M. (1980). The height of handwriting. *Acta Psychologica, 46,* 141–151.

Received May 17, 1992
Revision received July 21, 1993
Accepted February 14, 1994 ■